

LAER-MoE: Load-Adaptive Expert Re-layout for Efficient Mixture-of-Experts Training

Xinyi Liu*
 Peking University
 Beijing, China
 xy.liu@stu.pku.edu.cn

Yujie Wang*
 Peking University
 Beijing, China
 alfredwang@pku.edu.cn

Fangcheng Fu†
 Shanghai Jiao Tong
 University
 Shanghai, China
 ccchengff@sjtu.edu.cn

Xuefeng Xiao
 Bytedance Seed
 Beijing, China
 xiaoxuefeng.ailab@bytedance.com

Huixia Li
 Bytedance Seed
 Beijing, China
 lihuixia@bytedance.com

Jiashi Li
 Bytedance Seed
 Shenzhen, China
 lijiashi@bytedance.com

Bin Cui*‡
 Peking University
 Beijing, China
 bin.cui@pku.edu.cn

Abstract

Expert parallelism is vital for effectively training Mixture-of-Experts (MoE) models, enabling different devices to host distinct experts, with each device processing different input data. However, during expert parallel training, dynamic routing results in significant load imbalance among experts: a handful of overloaded experts hinder overall iteration, emerging as a training bottleneck.

In this paper, we introduce LAER-MoE, an efficient MoE training framework. The core of LAER-MoE is a novel parallel paradigm, Fully Sharded Expert Parallel (FSEP), which fully partitions each expert parameter by the number of devices and restores partial experts at expert granularity through All-to-All communication during training. This allows for flexible re-layout of expert parameters during training to enhance load balancing. In particular, we perform fine-grained scheduling of communication operations to minimize communication overhead. Additionally, we develop a load balancing planner to formulate re-layout strategies of experts and routing schemes for tokens during training. We perform experiments on an A100 cluster, and the results indicate that our system achieves up to 1.69x acceleration compared to the current state-of-the-art training systems. Source code available at <https://github.com/PKUDAIR/Hetu-Galvatron/tree/laer-moe>.

*School of Computer Science & Beijing Key Laboratory of Software and Hardware Cooperative Artificial Intelligence Systems, Peking University

†School of Artificial Intelligence, Shanghai Jiao Tong University

‡Institute of Computational Social Science, Peking University (Qingdao)

CCS Concepts: • Computing methodologies → Artificial intelligence; Distributed computing methodologies.

Keywords: Mixture-of-Experts, Load Balancing, Distributed Training, Expert Parallelism, Large Language Models

ACM Reference Format:

Xinyi Liu, Yujie Wang, Fangcheng Fu, Xuefeng Xiao, Huixia Li, Jiashi Li, and Bin Cui. 2026. LAER-MoE: Load-Adaptive Expert Re-layout for Efficient Mixture-of-Experts Training. In *Proceedings of the 31st ACM International Conference on Architectural Support for Programming Languages and Operating Systems, Volume 2 (ASPLOS '26), March 22–26, 2026, Pittsburgh, PA, USA*. ACM, New York, NY, USA, 19 pages. <https://doi.org/10.1145/3779212.3790180>

1 Introduction

Large Language Models (LLMs) have demonstrated remarkable capabilities across various tasks [2, 6, 19, 38, 39, 42, 43, 47, 52, 54]. However, the exponential growth in model parameters has led to significant computational and memory challenges in training these models [9]. Mixture of Experts (MoE) architectures have emerged as a promising solution, enabling the training of models with trillions of parameters while maintaining computational demands by activating only a subset of experts for each input token [3, 33]. Specifically, the feed-forward network (FFN) layers are typically replaced with MoE layers, which consist of a gating network and multiple FFNs, each representing a different expert. In an MoE layer, each token is routed by the gating network to only a few selected experts. The final output is computed as a weighted sum of the outputs from these selected experts.

Despite the computational advantages, the tremendous size of expert parameters often exceeds the memory capacity of individual devices. Therefore, expert parallelism [12, 16] is a widely used technique to facilitate distributed training of MoE models. In expert parallelism, each device stores only a subset of experts to reduce memory consumption, while other model parameters are replicated across all devices, with different training data allocated to each device. In each MoE layer, tokens are routed by the gating network to the



This work is licensed under a Creative Commons Attribution 4.0 International License.

ASPLOS '26, Pittsburgh, PA, USA

© 2026 Copyright held by the owner/author(s).

ACM ISBN 979-8-4007-2359-9/2026/03

<https://doi.org/10.1145/3779212.3790180>

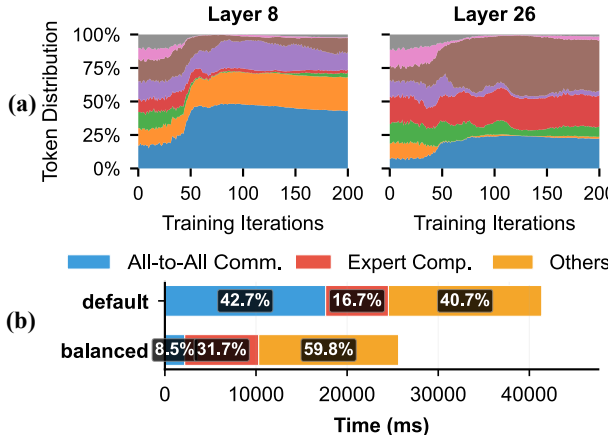


Figure 1. (a) Token distribution during training Mixtral 8x7B, showing significant imbalance. (b) Time breakdown, where “default” denotes the profiling result without auxiliary loss, and “balanced” denotes the result when enforcing fully balanced routing.

devices hosting the chosen experts. The outputs of experts are then sent back to the original device of each token.

Though expert parallelism alleviates the memory burden of a single device, it still faces critical challenges when employed for distributed training. The **dynamic and imbalanced routing distribution** during training creates significant load imbalances across devices, leading to substantial tail latency that severely impacts overall training efficiency [11, 29, 46]. For instance, Fig. 1(a) records the changes in routing distribution over time while training Mixtral 8x7B, showing that overloaded experts emerge almost at every training iteration, and the expert load dynamically fluctuates across iterations. Consequently, this imbalance leads to significant tail latency, as overloaded experts take longer to compute, causing other devices to wait. This is reflected in notable communication delays, as shown in Fig. 1(b). The imbalance in load causes the proportion of All-to-All communication time to increase from less than 10% to over 40%.

A notable line of efforts to address this challenge is to enforce load balance through algorithmic techniques like adding auxiliary losses [7, 16]. However, as we will empirically show in Sec. 2 and Sec. 5.2, algorithmic solutions substantially slow down training convergence [37]. Thus, this work concentrates on the system-level perspective.

Existing system-level load balancing methods mainly focus on how to adjust the *expert layout*, which can be generally categorized into expert replication and expert relocation. In vanilla EP (e.g., GShard [16]), expert placement is fixed throughout training. Expert replication techniques, such as FasterMoE [11] and Prophet [40], replicate high-load experts across multiple devices to mitigate imbalance. Expert relocation strategies, like SmartMoE [46], dynamically adjust expert placement based on historical routing distributions,

while FlexMoE [29] combines both approaches by dynamically adjusting expert replicas and their locations. However, these methods suffer from fundamental limitations.

Particularly, these optimizations introduce *additional re-layout overhead*, which *refrains existing methods from achieving load balance*. Expert replication requires additional communication for gradient synchronization of replicated experts. This communication is imbalanced because experts are not replicated across all devices. Expert relocation involves migrating expert parameters and optimizer states, which requires a communication volume typically 6x the size of the expert parameters. This substantial overhead causes larger peak memory due to the simultaneous allocation of send and receive buffers. Prior works treat re-layout as an individual phase, forcing a trade-off between load-balancing effectiveness and re-layout overhead. To manage such overhead, existing methods have to restrict themselves when adjusting the replication and/or relocation strategies. For instance, SmartMoE regulates relocation frequency to be low (e.g., hundreds of iterations), while Prophet and FlexMoE penalize adjustment strategies that will incur high overhead. As a result, existing methods fail to achieve timely, optimal adjustments in response to changes in routing distribution.

To fill this gap, our work explores optimizing expert re-layout strategies in response to dynamically changing routing distributions, while minimizing the impact from expert re-layout to achieve superior load balancing strategies. Given the dynamic nature of routing distributions, it is imperative for expert re-layout algorithms to swiftly adapt and adjust strategies. Moreover, when expert replication is involved in location strategies, it is essential to efficiently determine which replica each token should be routed to, necessitating rapid expert routing decisions. Our primary challenge lies in effectively managing the additional communication and devising enhanced load balancing algorithms, alongside designing efficient expert re-layout algorithms and corresponding routing strategies.

To tackle the challenges previously outlined, our work proposes LAER-MoE, a novel MoE training system leveraging *Load-Adaptive Expert Re-layout*. In contrast to prior works that treat re-layout as an isolated phase, LAER-MoE innovatively fuses re-layout with FSDP’s parameter prefetching and gradient reduce-scattering. This design enables re-layout at every iteration without additional memory cost and perfectly hides re-layout overhead, providing more flexible re-layout strategies and more immediate load-balancing responses to routing distribution changes. Specifically, we propose two key innovations to achieve this.

First, we combine the principles of fully sharded data parallelism (FSDP) [53] with expert parallelism (EP) to introduce a novel parallel paradigm termed Fully Sharded Expert Parallelism (FSEP). Unlike traditional EP, which allocates different experts to separate devices, FSEP fully shards each expert, with each device storing only a shard of all experts. During

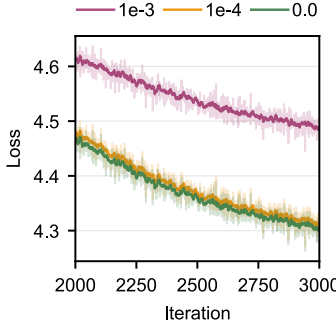


Figure 2. Loss curve with different auxiliary loss weights.

forward and backward propagation, each device gathers complete parameters of required experts. Moreover, FSEP fuses the expert re-layout process with the parameter pre-fetching and gradient reduce-scattering in FSDP, so that the re-layout overhead can be overlapped by the computation time of forward and backward passes. This offers much better flexibility for designing load balancing algorithms.

Second, we design an intelligent load balancing planner that dynamically monitors expert load during training and generates load-adaptive expert re-layout strategies and token routing results for each training iteration. Our planner employs heuristic greedy strategies to execute an asynchronous expert layout tuner that dynamically resolves expert layout strategies, coupled with a synchronous token dispatcher that rapidly determines expert routing strategies based on real-time training demands, achieving superior load balancing, free from the constraints imposed by re-layout overhead.

Based on the proposed new MoE parallel paradigm FSEP and the intelligent load balancing planner, we efficiently implement our system LAER-MoE atop PyTorch. Experiments demonstrate that LAER-MoE achieves up to 1.69 \times acceleration over state-of-the-art (SOTA) training systems. LAER-MoE’s ability to dynamically adjust expert layout during training without communication overhead makes it particularly effective for large-scale MoE model training.

The key contributions of this work include:

- We propose a novel MoE parallel paradigm FSEP, enabling flexible, in-training expert re-layout while masking re-layout communication overhead.
- We devise an intelligent load balancing planner that dynamically co-optimizes token routing and expert layout, achieving timely and effective adjustment.
- We develop an efficient MoE training system, namely LAER-MoE, delivering up to 1.69 \times end-to-end acceleration over existing SOTA systems.

2 Preliminary

Mixture of Experts. The core idea of Mixture of Experts (MoE) is to sparsely route input data to a subset of expert

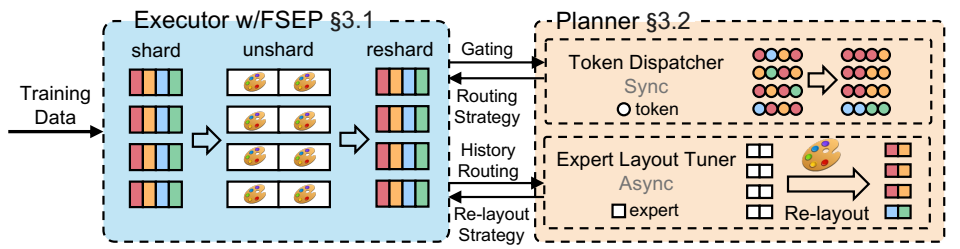


Figure 3. The overview of LAER-MoE.

networks and combine their outputs through a gating mechanism [33]. Specifically, given an input x , the output of an MoE model can be expressed as: $y = \sum_{i=1}^n g(x)_i \cdot f_i(x)$, where $g(x)_i$ is the output of the gating network representing the weight assigned to the i -th expert, $f_i(x)$ is the output of the i -th expert network, and n is the total number of experts. The gating function $g(x)_i$ is often implemented via a top-k selection followed by a softmax operation, i.e., $g(x) = \text{Softmax}(\text{TopK}(x \cdot W_g))$, where W_g is the weight of the gating network. This gating mechanism ensures that only a small number of experts (typically $k=1$ or $k=2$) are activated for each input.

Parallelism in Distributed MoE Training. MoE models typically contain far more parameters than dense LLMs, making distributed parallelism essential for efficient training.

Data parallelism (DP) [20, 49] splits data samples and replicates the entire model across devices, involving gradient synchronization during training. To avoid redundant parameter storage, Sharded Data Parallelism (SDP; e.g., DeepSpeed-Zero [31], PyTorch FSDP [53]) partitions parameters across devices while preserving DP semantics, enabling training larger models at the cost of extra communication for parameter gathering and gradient scattering. To overlap these communications with computation, PyTorch FSDP manages communication operations on separate CUDA streams. During forward passes, it prefetches parameters of the next layer while computing the current layer. Similarly, during backward passes, it synchronizes gradients of the previous layer while computing gradients for the current layer.

Expert parallelism (EP) [16] is designed for MoE models, where different experts are distributed across multiple devices, and each device hosts a subset of experts. Meanwhile, other non-expert modules are replicated and executed in DP-style. In each MoE layer, tokens are routed to devices containing the selected experts based on the routing results of the gating network. The output from the experts is then returned to the original device of the corresponding token. This process involves two communication operations: All-to-All dispatch and All-to-All combine.

Model parallelism (MP) splits the model parameters across multiple devices, which can be categorized into tensor parallelism (TP) [28] and pipeline parallelism (PP) [10, 26, 27]. TP splits the matrix multiplication computations across devices, utilizing communication to synchronize the computation outputs. PP partitions the model into stages with consecutive layers; each device computes its stage and forwards activations to the next via point-to-point communication.

Heterogeneous Expert Parallelism (HEP) [15, 21] is designed to address the load difference between the Attention and MoE layers in MoE models. The central idea is to employ distinct parallel strategies for these two types of layers, given their heterogeneous computational and communication characteristics. Specifically, the Attention layer typically performs dense computations, making it more suitable for TP. In contrast, the inherent sparse activation characteristic of MoE layers makes it more adaptable for EP.

Algorithmic Load Balancing Methods. To mitigate the imbalance issue, efforts have been made from the algorithmic perspective. Involving auxiliary losses is a typical approach to encourage balanced routing [7, 16], yet it inevitably impacts model convergence. Fig. 2 illustrates the convergence curves on Mixtral-8x7b using different auxiliary loss weights. It can be found that the increase in the auxiliary loss weight leads to a rise in the number of steps needed for the model to achieve equivalent performance. Some methods further consider discarding tokens to limit the load on each expert [12, 16], or directly modifying routing strategies for better balance [4, 17, 24, 32, 55]. However, these algorithmic approaches represent a trade-off between system efficiency and model quality, and often necessitate extensive experimentation for validation to adjust hyperparameters [8, 37]. Our work aims at tackling the imbalance issue from the system-level perspective.

System-level Load Balancing Methods. To maintain the training unaltered while balancing the load of different devices, existing works have proposed to adjust the expert layout over the devices in response to the dynamic routing distribution [11, 29, 40, 46]. Particularly, expert replication and expert relocation are two major techniques, where the former allows high-load experts to be hosted on multiple devices, while the latter dynamically adjusts the locations of experts. However, as introduced in Sec. 1, existing works suffer from the overhead caused by expert re-layout and compromise load balance.

3 System Design

Fig. 3 illustrates the main architecture of LAER-MoE, featuring an executor based on a novel parallel paradigm and a load-balancing planner. The planner dynamically monitors expert load during training and provides the executor with optimized expert re-layout strategies and specific routing

Table 1. Notations and Definitions used in this paper.

N	Number of devices
E	Number of experts
C	Expert capacity per device
P	Parallel dimensions
Ψ	Parameter sizes
$R_{i,j}$	Number of tokens on device i routed to expert j
$A_{i,j}$	Expert re-layout strategy
$S_{i,j,k}$	Token routing strategy
T	Time of the cost model
$V_{comm/comp}$	Communication/computation volume per token
$B_{inter/intra}$	Inter-node/intra-node bandwidth
B_{comp}	GPU computational power
F_{ckpt}	Checkpoint optimization flag
$bw(i, j)$	Bandwidth between devices i and j
$node(i)$	Node where device i is located

results. The executor then employs the new parallel paradigm to implement the updated expert re-layout strategy and routing results in real-time during training.

Specifically, we will first introduce the new parallel paradigm, Fully Sharded Expert Parallelism (FSEP), detailing its execution process, communication volume, and memory cost. For the planner, we outline our optimization objectives and propose a heuristic greedy strategy to execute an asynchronous expert layout tuner and a synchronous token dispatcher based on the real-time demands of training. For clarity, the frequently used notations are listed in Tab. 1.

3.1 FSEP: Fully Sharded Expert Parallelism

We first introduce the executor, which incorporates the new parallel paradigm FSEP, inspired by EP and FSDP, allowing more flexible retrieval of expert parameters during training.

Workflow of FSEP. The fundamental concept of FSEP involves dividing experts into chunks with equal size, corresponding to the number of devices, with each device retaining a distinct chunk from each expert. During training, devices restore entire expert parameters through All-to-All communication. When restoring parameters, each device does not need to acquire the complete parameters for all experts. Instead, similar to EP, each device restores full parameters from different experts.

Formally, for N devices and E experts, each device has an expert capacity C (the number of complete expert parameters restored), each device stores E chunks, each of size $\frac{1}{N}$ experts, and restores C complete expert parameters during forward and backward. Fig. 4 illustrates such an example, where $N = 4$, $E = 4$, $C = 2$. This paradigm mirrors the memory efficiency and initialization approach of FSDP, while during training, it exhibits parallelism similar to EP. Thus, we designate this new parallel paradigm as fully sharded expert parallelism (FSEP). Furthermore, due to the uniform nature of the communication during restoration, each device

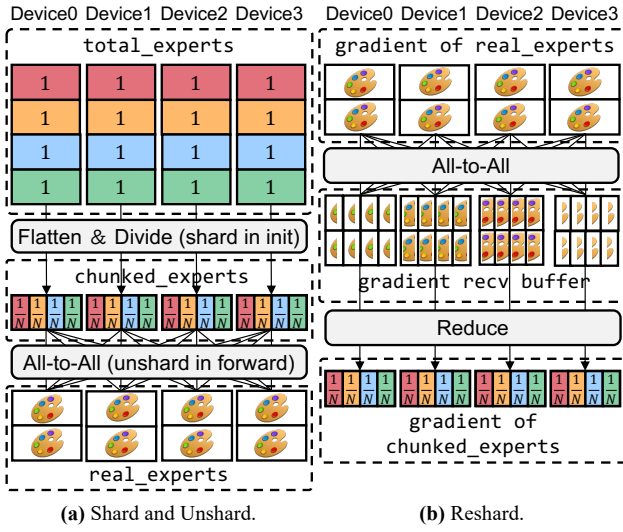


Figure 4. Illustration of FSEP, where $N = 4$, $E = 4$, $C = 2$.

can acquire an **arbitrary layout** of experts, significantly facilitating the application of load balancing methods, which will be discussed in Sec. 3.2.

To enhance the distributed training of MoE models and mitigate bottlenecks associated with new parallel strategies, FSEP must address a key challenge: *How to seamlessly integrate FSEP with existing parallel paradigms, enabling practitioners to easily adopt and transition to the new strategy?*

To tackle this challenge, we draw inspiration from methods in FSDP and refine the existing FSDP codebase. To implement unique partitioning logic of FSEP, we introduce three additional sharding methods: **shard**, **unshard**, and **reshard**, as depicted in Fig. 4.

Shard is invoked during model initialization. Similar to traditional FSDP, we treat all expert parameters in the MoE layer as a single unit, and the shard operation is conducted at this level. During model initialization, the parameters of each expert are flattened and concatenated into a large parameter, which is then evenly divided into N chunks, with each device retaining a distinct chunk. These E partitioned parameters are subsequently concatenated for further management.

Unshard is utilized during forward or backward passes to restore complete parameters of the needed experts. Since it is unnecessary to acquire all expert parameter information, unshard employs the All-to-All communication operator to obtain the parameters of specified experts.

Reshard is primarily used to revert parameters to their partitioned form. Since unshard does not release the sharded parameters, no additional operations are required here. However, reshard involves re-partitioning and synchronizing complete expert gradients post-backward computation, employing the All-to-All communication operator for gradient synchronization. Specifically, each expert gradient is divided

into N chunks, which are then sent to corresponding devices for reduction operations, as shown in Fig. 4(b).

It is crucial to note that, in traditional FSDP, shard stores the shape of each parameter before flattening as meta information. During unshard, parameters are restored to their unflattened form using split and view operations based on this meta-information, ensuring the correct functioning of the autograd engine of PyTorch. In contrast, FSEP requires flattening all expert parameters during shard, yet only restores C expert parameters during unshard, leading to mismatched meta-information. To address this, we employ an architecture separating flattened parameters from meta-information, as illustrated in Fig. 4(a). During shard, we flatten the parameters in **total_experts** but record the meta-information of **real_experts**, allowing parameters to be accurately restored during unshard, and enabling direct computation using methods in **real_experts** during forward computation.

Moreover, it is important to emphasize that FSEP maintains numerical precision identical to FSDP, with no loss in accuracy. This is because FSEP only modifies the parameter storage and communication patterns during sharding and unsharding operations, while the actual forward and backward computations remain unchanged.

Communication Optimizations. Employing FSEP introduces significant communication overhead. To mitigate this, we implement fine-grained scheduling to obscure this overhead, as shown in Fig. 5. Specifically, the incurred overhead encompasses three operations: All-to-All communication to restore complete expert parameters during unsharding in both forward and backward passes, and gradients resharing and synchronization post-backward computation.

Regarding the communication introduced by unshard, similar to FSDP, we incorporate parameter prefetching in the executor. Contrasting traditional methods that prefetch the parameters of the next unit, within the context of heterogeneous parallelism, this involves prefetching expert parameters during attention computation, resulting in suboptimal overlap effects, as shown in Fig. 5(a). To address this, we relax the prefetching constraints, overlapping the expert computation of the current layer with the prefetching of expert parameters for the next layer, allowing the more computationally demanding expert computation to obscure the prefetching communication, as depicted in Fig. 5(b). We further schedule the prefetching communication alongside the All-to-All communication in the token dispatcher, ensuring the former is launched after the latter has concluded, thus reducing potential channel contention, as shown in Fig. 5(c).

For the communication introduced during resharing, traditional methods rely on the autograd engine to automatically schedule gradient communication, leading to uncontrollable communication timing and overlap effects. To address this, we design a gradient communication delay method, postponing this communication operation when the autograd engine is prepared, deferring it to the subsequent expert

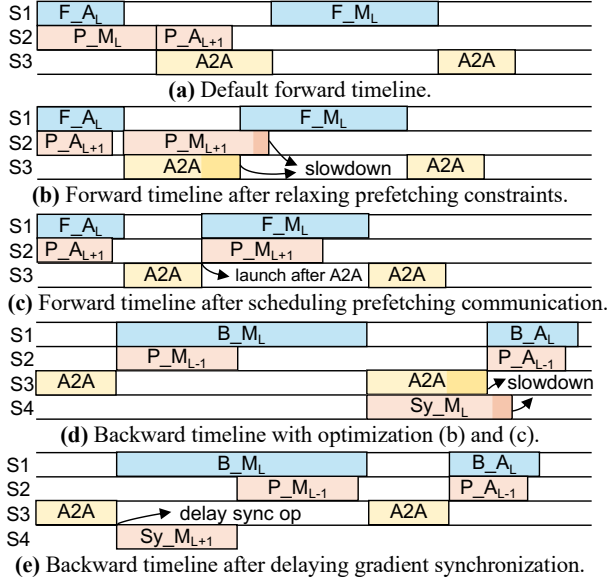


Figure 5. Communication optimization in FSEP, where A represents Attention layer, M represents MoE layer, S represents Stream, blue blocks on S1 represent forward and backward computation (F and B), yellow blocks on S3 represent All-to-All communication of token dispatcher (A2A), and red blocks on S2 and S4 represent prefetching communication (P) and gradient synchronization (Sy).

layer's backward computation to ensure optimal overlap effects, as illustrated in Fig. 5(e).

Communication and Memory Analysis. To demonstrate the effectiveness of the executor, we provide a quantitative analysis of communication volume and memory usage.

Communication Analysis. In FSEP, the communications for shard and reshards are inverse, hence the communication volumes for these operations are consistent. Taking shard as an example, the parallel dimension of FSEP is $P_{fsep} = N$, and the size of each expert parameter is Ψ_{expert} . In each operation, each device needs to send C chunks of $\frac{1}{P_{fsep}}$ of expert parameters to other devices, while receiving C chunks it requires from each of them, leading to a communication volume of $V_{fsep} = C \times (P_{fsep} - 1) \times \frac{1}{P_{fsep}} \times \Psi_{expert}$ per device. The send/receive volumes between any pair of devices are identical. This constitutes a regular, balanced All-to-All communication operation, which achieves the same speed as standard All-to-All communication without incurring additional overhead. For the traditional FSDP+EP parallel paradigm, suppose the parallel sizes for EP and FSDP are P_{ep} and P_{fsdp} respectively, when model states and activation values are similar, these dimensions satisfy $P_{ep} \times P_{fsdp} = N$, $C \times P_{ep} = E$. During unshard operation of FSDP, each device uses Allgather to aggregate C complete expert parameters across devices within the same FSDP communication group, resulting in a communication volume of $V_{fsdp} = \frac{P_{fsdp} - 1}{P_{fsdp}} \times C \times \Psi_{expert}$. The

ratio of communication volumes between the two methods is $\frac{V_{fsep}}{V_{fsdp}} = \frac{(P_{fsep} - 1) \times P_{fsdp}}{P_{fsep} \times (P_{fsdp} - 1)}$. As the cluster size increases, this ratio approaches 1. For instance, when $P_{fsep} = 32$, $P_{ep} = 4$, $P_{fsdp} = 8$, $\frac{V_{fsep}}{V_{fsdp}} \approx 1.1$. Compared to traditional paradigms, FSEP incurs only trivial additional communication overhead. Furthermore, through the fine-grained communication scheduling outlined in Fig. 5, this communication can be overlapped with computation, enabling FSEP to provide dynamic expert re-layout opportunities while retaining overhead similar to the traditional paradigm.

Memory Analysis. To understand the impact of FSEP on model state, we analyze a classic scenario: the MoE layer employs FSEP, whereas other modules utilize equivalently sized FSDP. The model state primarily consists of optimizer state, parameter state, and gradient state. For the optimizer state, since these parallel paradigms are fully sharded, the optimizer state is $\frac{1}{P_{fsep}}$ of the full optimizer state. Taking the total parameter size of the complete model as Ψ_{all} , and the size of parameters excluding expert parameters for each Transformer layer as Ψ_{other} , following the communication optimization in Fig. 5, all parameters for the next layer are prefetched during the expert computation of current layer, leading to a parameter state overhead of $\frac{\Psi_{all}}{P_{fsep}} + \Psi_{other} + 2 \times C \times \Psi_{expert}$. Furthermore, we delayed gradient updates, so the gradient state overhead is consistent with the parameter state. Compared to traditional FSDP, our method incurs only an additional $2 \times C \times \Psi_{expert}$ in memory overhead, arising from parameter and gradient states. Relative to the full model, this additional memory is negligible. As for other types of parallel paradigms, they often fail to achieve fully sharded parameter and gradient states, making FSEP a memory-efficient parallel paradigm. Notably, this additional memory overhead is attributed to the communication optimizations detailed in the previous section, not to the FSEP mechanism itself. Traditional FSDP can similarly incorporate these aforementioned communication optimizations to enhance training efficiency, in which case both FSDP and FSEP exhibit identical memory footprints.

Computation-Communication Overlap Analysis. To validate the feasibility of overlapping parameter prefetching with expert computation, we provide a theoretical analysis of an MoE layer employing a SwiGLU MLP with bfloat16 precision. Let H denote the hidden dimension, H' the intermediate dimension, K the top- k selection in the router, and S the total token count per device in each micro-batch.

Under the assumption of balanced loading, the computation workload per device is $S \cdot K \cdot (6 \cdot H \cdot H')$, where the parenthesized term indicates the per-token FLOPs for SwiGLU. The communication volume for prefetching (sending and receiving, respectively) by each device is $3 \cdot C \cdot H \cdot H' \cdot \text{sizeof(bfloat16)}$. Consequently, computation latency masks communication

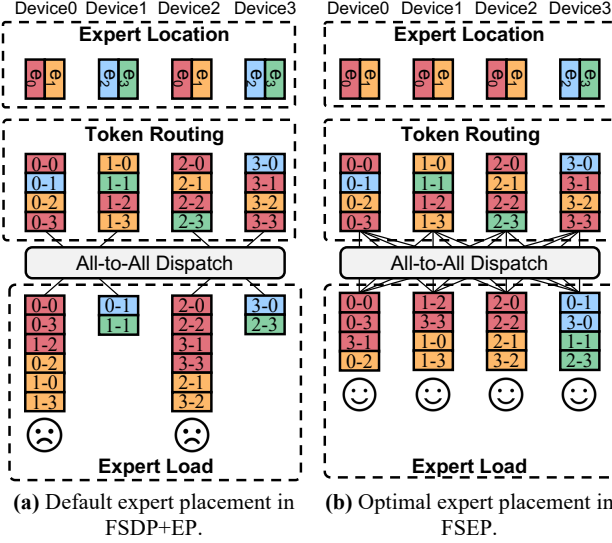


Figure 6. The opportunities of load balancing in FSEP.

overhead provided that the following condition holds:

$$S > (C \cdot V_{comp}) / (K \cdot V_{comm}) \quad (1)$$

In our experimental setup (detailed in Sec. 5.1), the condition in Eq. 1 is theoretically satisfied when $S \geq 17K$. Empirically, we observe that $S = 16K$ suffices to achieve effective overlap, as the practical computation time often exceeds the theoretical lower bound due to load imbalance. Such a threshold is readily attainable in production scenarios [21, 56].

3.2 Load Balancing Planner

This section introduces the load balancing planner associated with the FSEP parallel paradigm, encompassing optimization opportunities presented by the new parallel paradigm, cost modeling, and a heuristic efficient load balancing solution method proposed based on training characteristics.

Optimization Opportunities. The major advantage offered by FSEP is the ability to freely select which experts are restored on each device during unshard. This allows for the strategic planning of expert re-layout strategies for each iteration, including the number of replicas for each expert and the device where each expert should be restored. Fig. 6 illustrates such an example: in a traditional setup with $N = 4$ and $P_{fsdp} = P_{ep} = 2$, experts 0 and 1 are fixed to be restored on devices 0 and 2, while experts 2 and 3 are fixed on devices 1 and 3. However, the actual routing distribution is significantly skewed, with tokens for experts 0 and 1 significantly outnumbering those for other experts, leading to overloading on devices 0 and 2 and underloading on devices 1 and 3. With FSEP, it is possible to flexibly adjust the experts restored on device 1 to be experts 0 and 1, subsequently routing part of the tokens for experts 0 and 1 to device 1 for computation, and shifting tokens originally sent to device 1 to device 3,

thereby achieving load balancing. Thus, FSEP can dynamically alter expert re-layout strategies based on real-time load, promoting load balance across devices, reducing tail latency, and ultimately accelerating training speed.

Problem Formulation. In the MoE training process, the execution time of the MoE layer is determined by the All-to-All communication for routing distribution and expert computation. Therefore, when modeling the load balancing problem, it is essential to consider both computation and communication costs. Formally, given $R_{i,j} \in \mathbb{N}^{N,E}$, where $R_{i,j}$ represents the number of tokens on device i routed to expert j , expert capacity limit C , inter-node communication bandwidth B_{inter} , intra-node communication bandwidth B_{intra} , communication volume per token V_{comm} , computational power of each GPU B_{comp} , and computation volume per token V_{comp} . We define the expert re-layout strategy $A_{i,j} \in \{0, 1\}^{N,E}$ and token routing strategy $S_{i,j,k} \in \mathbb{N}^{N,E,N}$, where $A_{i,j} = 1$ indicates expert j is placed on device i , and $A_{i,j} = 0$ otherwise. $S_{i,j,k}$ represents the number of tokens on device i routed to expert j that need to be sent to device k . The optimization goal is to minimize the total time, encompassing both communication and computation time.

To model the communication time, we need to calculate the total cost of All-to-All communication. In particular, we consider the point-to-point communication cost for each pair of devices based on the topology and sums them up, i.e., $T^{comm} = 4 \times V_{comm} \sum_{i,j,k} \frac{S_{i,j,k}}{bw(i,k)}$, where $bw(i, k)$ represents the intra- or inter-node bandwidth between devices i and k , and the multiplier is 4 since the forward and backward passes of an MoE layer involve four All-to-All communication operations in total.

To model the computation cost, which involves the forward and backward computation time, it is common practice to treat the backward cost as twice the forward one. Meanwhile, due to the imbalance issue, we need to find the maximum computation time across all devices. Thus, we model the computation cost as $T^{comp} = (3 + F_{ckpt}) \times \max_i T_i^{fw_comp}$, where $F_{ckpt} \in \{0, 1\}$ indicates whether activation checkpointing (a.k.a. recomputation) is used, and $T_i^{fw_comp}$ denotes the forward computation time on device i . Specifically, it is calculated as $T_i^{fw_comp} = V_{comp} \times \sum_{j,k} \frac{S_{k,j,i}}{B_{comp}}$.

Based on these, we propose a joint optimization problem:

$$\arg \min_{A_{i,j} \in \{0,1\}^{N,E}, S_{i,j,k} \in \mathbb{N}^{N,E,N}} T = T^{comm} + T^{comp} \quad (2)$$

$$\text{s.t. } \sum_i A_{i,j} = C \quad \forall j \in [0, E-1] \quad (3)$$

$$\sum_k S_{i,j,k} \times A_{k,j} = R_{i,j} \quad \forall i, j \in [0, N-1] \times [0, E-1] \quad (4)$$

The constraint 3 limits the number of experts placed on each device, while the constraint 4 guarantees that all tokens are routed to the correct experts.

Algorithm 1: Expert Relocation Algorithm

Input: $expert_rep$, $expert_loads$, N , E , C
Output: A

```

1  $expert\_count, device\_loads \leftarrow zeros(N), zeros(N);$ 
2  $A, list \leftarrow zeros(E, N), [];$ 
3 for  $i \in [0, E - 1]$  do
4    $list.extend([(i, \frac{expert\_loads[i]}{expert\_rep[i]}) \times expert\_rep[i]);$ 
5  $list \leftarrow DescendingSortByLoad(list);$ 
6 for each  $(expert, load)$  in  $list$  do
7    $node\_cnt \leftarrow$  count replicas of  $expert$  per node;
8    $min\_node \leftarrow \min(node\_cnt);$ 
9    $available \leftarrow \{i : expert\_count[i] < C \wedge node(i) \in min\_node\};$ 
10   $device \leftarrow$  select from  $available$  with min load;
11   $A_{expert, device} \leftarrow A_{expert, device} + 1;$ 
12   $device\_loads_{device} \leftarrow device\_loads_{device} + load;$ 
13   $expert\_count_{device} \leftarrow expert\_count_{device} + 1;$ 
14 return  $A$ ;
```

Solving Algorithm The formulated joint optimization problem is a nonlinear integer programming (NIP) problem, which is hard to solve within polynomial time and typically requires existing solvers such as SCIP [1] to find approximate solutions. Moreover, the problem involves $N^2 \times E + N \times E$ variables, and as the problem size expands, the solver’s time consumption grows exponentially. In traditional EP, tokens are simply routed to the device hosting the corresponding expert. However, FSEP permits expert replication, necessitating additional decisions regarding which replication of the corresponding expert each token should be routed to. Additionally, there is a strict sequential dependency between the token routing strategy and All-to-All dispatch communication, indicating that token communication dispatch can only proceed once the specific token routing strategy is established. Therefore, it is crucial to derive the specific routing strategy as quickly as possible. Consequently, directly solving this joint optimization problem is unsuitable. To tackle this, we propose a method that separates expert re-layout strategies from token routing strategies. We begin by crafting a token dispatcher that employs a lite routing algorithm based on the immediate dependency of routing strategies. Subsequently, we design a heuristic greedy algorithm to solve the expert re-layout strategy based on the lite routing, serving as our expert layout tuner.

Token Dispatcher. As experts may be replicated, the primary issue in token routing is determining which replica of the expert each token should be routed to. Our algorithm is inspired by the following two considerations: 1) In modern training clusters, intra-node communication speeds frequently surpass inter-node communication speeds. Therefore, the routing policy should minimize inter-node token transfers. 2) Fine-grained control over the total number of

Algorithm 2: Expert Layout Algorithm

Input: R, N, E, C, ϵ : The size of replicas_set
Output: A

```

1  $replicas\_set \leftarrow \emptyset;$ 
2  $replicas\_set.append(replica\_allocation(R, N, E, C));$ 
3  $evenly\_replicas \leftarrow [\frac{N \times C}{E}] \times E;$ 
4  $replicas\_set.append(evenly\_replicas);$ 
5 while  $\text{len}(replicas\_set) < \epsilon$  do
6    $rand\_rep \leftarrow$  randomly select from  $replicas\_set$ ;
7    $replicas\_set.append(\text{random perturb of } rand\_rep);$ 
8    $expert\_load \leftarrow R.sum(axis = 0);$ 
9    $best\_A, best\_S, best\_T \leftarrow None, None, +\infty;$ 
10  for each  $replicas$  in  $replicas\_set$  do
11     $A \leftarrow expert\_relocation(replicas, R, N, E, C);$ 
12     $S \leftarrow lite\_routing(R, A, N, E, C);$ 
13     $T \leftarrow time\_cost(A, S);$ 
14    if  $T < best\_T$  then
15       $best\_A, best\_S, best\_T \leftarrow A, S, T;$ 
16 return  $best\_A$ ;
```

tokens received by each device requires coordination among all devices, resulting in additional communication overhead, which is inefficient. Thus, we design a greedy-based lite routing algorithm, which is topology-aware and requires no global routing information, only global expert layout information. Specifically, for each expert, if replicas exist within the node, tokens routed to the expert are evenly distributed among all replicas within the node. If no replicas exist within the node, tokens are evenly distributed among all replicas across global nodes. We detail the lite routing algorithm in Appendix B.

Expert layout tuner. We now introduce how to solve the expert re-layout strategies using a heuristic greedy approach. Specifically, the problem is divided into two steps: first determining the number of replicas for each expert, and then solving the location of these replicas.

For determining the number of replicas, an intuitive approach is to allocate replicas based on the expert’s load: experts with higher loads receive more replicas, while those with lower loads receive fewer. Accordingly, we propose a priority-queue-based replica allocation method. It detects the expert with the highest average load (i.e., the ratio of actual load to the number of replicas) and expands the number of replicas for this expert until the total number of replicas meets the requirement. We illustrate the detailed expert replica allocation algorithm in Appendix C.

For solving expert relocation, we develop a greedy relocation method which is topology-aware and designed with the lite routing strategy to ensure that expert replicas are balanced across different nodes, as detailed in Alg. 1. First, we calculate the average number of tokens each replica of an expert needs to process, then sort all these replicas in

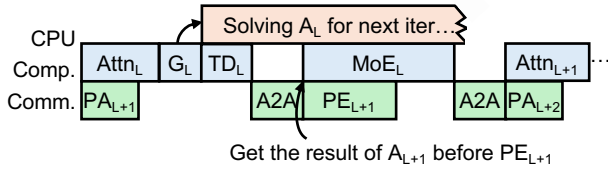


Figure 7. The overall workflow of LAER-MoE.

descending order (Line 3-5). Next, we sequentially select devices for each replica. Since tokens are evenly distributed across all replicas within a node during routing, it is crucial to ensure that the number of replicas of the same expert within each node is as balanced as possible. Therefore, for each replica, we first select the set of nodes with the fewest replicas of the current expert (Line 7-9), and then choose the device with the least total load within these nodes as the location of this replica (Line 10-13).

Additionally, since this replica number determination method may not guarantee optimality, we introduce a new scheme: assigning the same number of replicas to all experts based on the total number of replicas (Line 3). On top of these two allocation schemes, we introduce randomized perturbations to construct a set of replica schemes (Line 5-7). We then perform location solving for each scheme in the set sequentially, selecting the optimal strategy as the final solution (Line 9-15). The final solving process is depicted in Alg. 2.

3.3 Overall Workflow

Fig. 7 illustrates the overall workflow of LAER-MoE, where $Attn_L$, MLP_L , G_L and TD_L represent the attention layer, MLP in MoE layer, gate layer and token dispatcher of the L -th Transformer layer, respectively. PA_{L+1} and PE_{L+1} represent the prefetching of attention parameters and expert parameters for the $L + 1$ -th Transformer layer. As solving the expert re-layout strategy does not require high immediacy and requires certain time consumption, we delegate this process to the CPU side. During a training process, when computing the current MoE layer, the system first retrieves routing information of the current layer, then dispatches this routing information along with historical data from previous iterations to the expert layout tuner on the CPU side. The CPU references these data to generate new expert re-layout strategies for the next iteration of the layer. Meanwhile, the token dispatcher is employed on the GPU side for rapid token routing to facilitate subsequent All-to-All dispatch operations. After the All-to-All dispatch operation, the re-layout strategies for the next MoE layer’s experts are first retrieved from the CPU, and then the parameters for the next MoE layer are prefetched according to these strategies. This prefetch occurs concurrently with MLP computation. This mechanism continues iteratively layer by layer, organically integrating the executor with FSEP and the load balancing planner.

4 Implementation

LAER-MoE, inspired by Megatron’s implementation, extends support for the MoE architecture upon Galvatron [23, 25, 41], which accommodates various hybrid parallel strategies, including FSDP. LAER-MoE expands this foundation with approximately 11k lines of additional Python, CUDA, and C++ code. Furthermore, we employ the following methods to further optimize the training process.

Heterogeneous Parallel Strategy and Fine-Grained Recomputation

Our system also introduces heterogeneous parallel strategies. Specifically, for a Transformer layer, FSEP treats the complete expert parameters as a unit, while other parameters in the same layer are placed in another unit. This allows for independent parallel strategy selection, offering more flexible training options. Additionally, we introduce fine-grained recomputation, which can be performed at the granularity of Attention layers and MLP layers. For the MoE layer, we also provide the option to recompute only the expert computation part, preventing extra All-to-All communication overhead during recomputation.

Customized All-to-All Kernel. During expert parameter prefetching and gradient synchronization, the inflexibility of torch’s all-to-all communication interface results in additional memory for send/receive buffers and extra memory rearrangement overhead. To address this, we develop a custom communication kernel using CUDA to perform All-to-All communication directly between sharded and unsharded parameters, thereby reducing additional overhead. Crucially, this custom kernel is designed specifically to avoid memory overhead rather than to improve communication efficiency. It has identical efficiency to standard APIs under the same communication volume.

Host Bound Optimization. During MoE training, numerous CPU-blocking operations are encountered, such as the `masked_select` operation during traditional token rearrangement and host-to-device and device-to-host operations involved in interactions with the CPU-side solver. These operations can block the CPU, delaying subsequent GPU kernel launch instructions and impacting GPU utilization. To address this, we modify all host-to-device and device-to-host operations to be asynchronous and orchestrate synchronization timing to ensure correctness and efficiency. Specifically, we employ dedicated CUDA streams for H2D and D2H transfers, and explicit synchronization is performed on the respective streams only when the data is strictly required. This design ensures that the overhead from these operations is negligible. Additionally, we develop a triton kernel for token rearrangement, avoiding the use of torch operations that can cause blocking.

Efficient Solver of the Planner. In the planner, token routing demands immediacy, and the solving of expert re-layout strategies must be executed rapidly to ensure scalability. Consequently, we develop an efficient Triton kernel for

Table 2. Configurations of the evaluated models.

Model	Layers	Params	Activs	E&K
Mixtral-8x7B	32	46.70B	12.88B	8&2
Mixtral-8x22B	18	45.46B	12.86B	8&2
Qwen-8x7B	32	46.69B	12.88B	8&2
Mixtral-8x7B	24	35.09B	9.73B	16&4
Mixtral-8x22B	14	35.46B	10.09B	16&4
Qwen-8x7B	24	35.09B	9.73B	16&4

the token routing algorithm, ensuring rapid execution on the GPU. For solving expert re-layout strategies, we create an efficient C++ core and employ a multiprocess approach, utilizing a separate process to interact with the executor.

5 Experiments

5.1 Experimental Setups

Baseline Systems. We compare our system with Megatron [21], the state-of-the-art distributed training framework supporting MoE models. Megatron supports heterogeneous expert parallelism for flexible strategy combinations. Additionally, for a comprehensive comparison, we extended EP based on Torch FSDP as another baseline training framework with a fully sharded model state. Specifically, this configuration applies both FSDP and EP to MoE layers while utilizing FSDP for non-MoE layers, as employing standalone EP on MoE layers results in Out-of-Memory (OOM) errors due to insufficient parameter sharding. Furthermore, we incorporate the communication optimizations detailed in Sec. 3.1 into this FSDP+EP baseline, thereby isolating and highlighting the efficacy of our approach in addressing load imbalance. We also compare our approach with FlexMoE [29], which is currently the state-of-the-art load balancing strategy employing expert replication.

Hardware Environments. We conduct our experiments on a 4-node GPU cluster, with each node containing 8 NVIDIA A100 80GB GPUs. Within nodes, GPUs within a node are connected via NVLink, and nodes are interconnected via Infiniband. The peak unidirectional communication bandwidth intra-node is 300 GB/s, and inter-node is 800 Gbps.

Experimental Workloads. We experiment on three different model architectures: Mixtral-8x7B, Mixtral-8x22B [13], and additionally, transform Mixtral-8x7B into the Qwen-8x7B model architecture [44]. Besides the standard configuration of 8 experts with topk being 2(e8k2), we expand these models into configurations of 16 experts with topk being 4(e16k4), without altering the parameter count and computational load per layer. The specific model architectures, total parameter counts, and activated parameter counts are detailed in Tab. 2, where E&K denotes the number of experts and topk. We utilize the complete Mixtral-8x7B and Qwen-8x7B model for the e8k2 series models, while Mixtral-8x22B has some layers reduced due to memory constraints. For

the e16k4 series models, as their activations occupy more memory during training, we partially reduce some layers of all three model architectures. We set the expert capacity per device C to 2 for the e8k2 series models, and 4 for the e16k4 series models. We conduct our training using a dropless approach and employ Wikitext and C4 as our datasets. In our experiments, the key hyperparameters influencing efficiency are global batch size, sequence length, and auxiliary loss weight. Other hyperparameters (e.g., learning rate, weight decay) do not fundamentally alter the efficiency. Accordingly, we specify sequence length and auxiliary loss weight (default is 0) in each experiment, while maintaining the standard LLM training configuration for other parameters.

5.2 End-to-End Performance

We evaluate all systems at 8K context across all models and datasets: 20-step warmup, then the average of the next 50 iterations. We also compare the impact of auxiliary loss on our method, contrasting no auxiliary loss with using Switch-Transformer auxiliary loss, with a weight of 1e-4. Megatron and FSDP+EP are manually tuned to their optimal parallel strategies. For FlexMoE (no open-source release), we reproduce its scheduler and replace our expert re-layout planner, comparing it in conjunction with FSEP. As shown in Fig. 8, in all scenarios, LAER-MoE consistently outperformed other methods, achieving up to 1.69 \times acceleration over Megatron and 1.50 \times over FSDP+EP. Compared to FlexMoE, LAER-MoE achieves a speedup of up to 1.39 \times , with an average improvement of 1.20 \times .

We first compare LAER-MoE with SOTA systems. As shown in Fig. 8, FSDP+EP performs better on e8k2 series models, while Megatron excels with e16k4 series models. For e8k2 series models, the larger parameter size results in higher model states memory, requiring Megatron to use a larger TP in attention layer to meet memory limits, hurting efficiency; FSDP+EP benefits from fully sharding, using the saved model states memory to increase tokens per micro-batch, thus outperforming Megatron. For e16k4 series models with slightly fewer parameters, Megatron is allowed to use a smaller TP for improved efficiency, surpassing FSDP+EP. Both baselines, however, suffer from expert-load imbalance issue, which inflates MoE tail latency, hurting overall efficiency. LAER-MoE addresses this by dynamically adjusting the expert layout during training, balancing token computation across devices and alleviating tail latency, achieving optimal results.

Next, we compare LAER-MoE with FlexMoE. FlexMoE attains strong speedups on e8k2 models but weaker gains on e16k4. This is because e8k2 models have fewer experts, allowing FlexMoE's iterative search to find a relatively optimal expert layout quickly, whereas the larger expert space on e16k4 models limits the quality of its solutions. Besides, FlexMoE considers the extra adjustment cost and penalizes layout changes, thereby excluding potentially optimal solutions. In contrast, LAER-MoE directly adjusts the expert

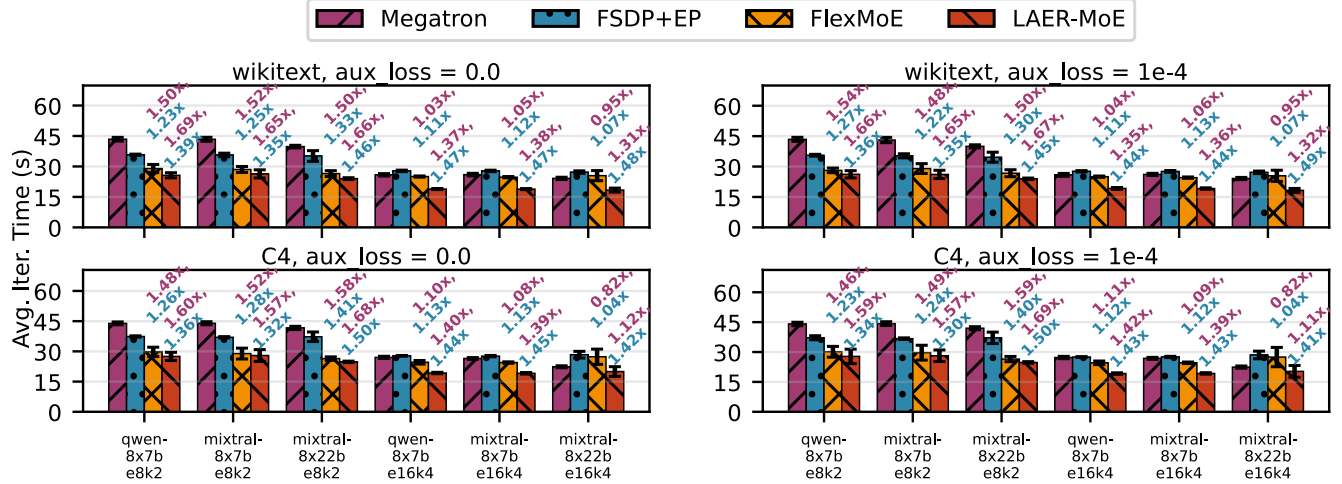
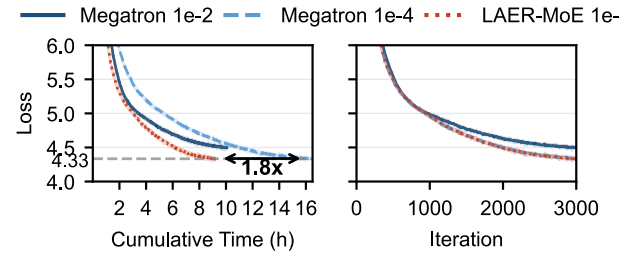
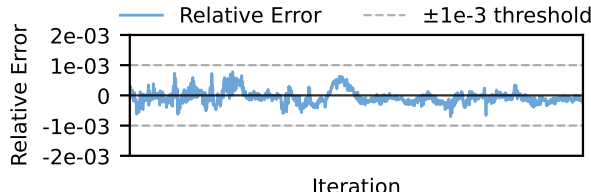


Figure 8. End-to-end performance under various model architectures for specific auxiliary loss weights and datasets, as depicted in the subfigures. Speedup ratios compared to Megatron (blue, top) and FSDP+EP (purple, bottom).



(a) Loss curves over training time (left side) and over training steps (right side) with different auxiliary loss weights.



(b) Relative error between LAER-MoE and Megatron with an auxiliary loss weight of 1e-4.

Figure 9. Convergence study on Mixtral-8x7B e8k2.

layout each step, offering greater flexibility and consistently achieving better results. Note that our FSEP paradigm is decoupled from load balancing solvers, allowing compatibility with any form of planner without imposing additional constraints, enabling the planner to provide more flexible expert layouts for better results. We also aim to develop more efficient and effective planners as part of our future work.

Last but not least, we conduct convergence experiments on Mixtral-8x7B e8k2 with 4K sequence length. We set LAER-MoE's weight of auxiliary loss to 1e-4 and compare it with

Megatron using 1e-2 and 1e-4 as the weight of auxiliary loss. As shown in Fig. 9(a), with an auxiliary loss of 1e-4, our system converges at the same rate as Megatron (relative error $< 1e-3$, see Fig. 9(b)), demonstrating its correctness. Coupled with the numerical precision guarantees detailed in Sec. 3.1, this convergence behavior confirms that FSEP incurs no loss in training precision. Besides, although training with auxiliary loss of 1e-4 requires fewer iterations than 1e-2, Megatron's 1e-2 auxiliary loss weight improves routing load balance, resulting in faster iterations than 1e-4, thus achieving faster convergence. However, LAER-MoE can train rapidly with an auxiliary loss of 1e-4, achieving the best convergence speed.

5.3 Case Study

To clearly analyze the optimization sources of LAER-MoE, we conduct an in-depth case study on Mixtral-8x7B for certain iterations using the Wikitext dataset. We break down the end-to-end time (averaged across all ranks), highlighting the All-to-All component, as shown in Fig. 10(a). The breakdown reveals that the speedup mainly comes from the acceleration of All-to-All communication, while expert computation and others (including attention computation and memory operations before and after All-to-All) have similar times across different methods. For FSDP+EP, due to tail latency from load imbalance, All-to-All communication time reached up to 40%. FlexMoE reduces this proportion through load balancing methods, while LAER-MoE achieves a reduction of All-to-All communication to below 20% by employing a more flexible load balance planner, resulting in up to a 2.68 \times speedup in All-to-All communication compared to the baseline. This evidence validates that our approach effectively facilitates load balancing, thereby translating directly into

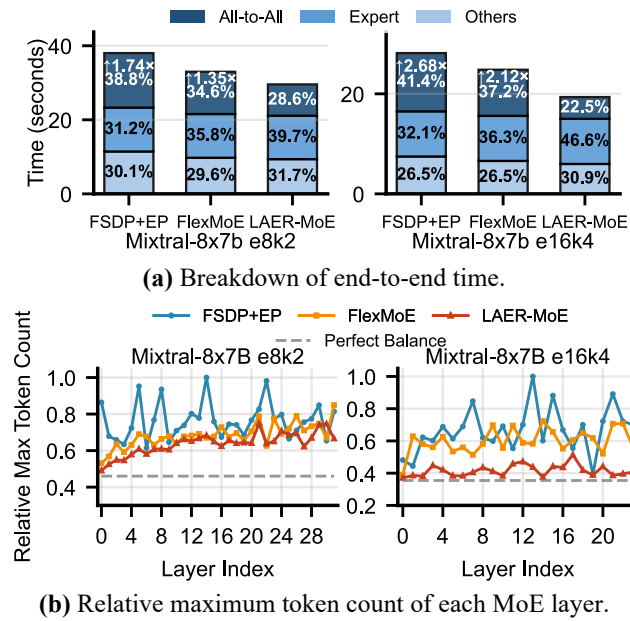


Figure 10. Case study of breakdown and maximum token count.

enhanced training efficiency. Regarding the breakdown details, the “Others” component primarily consists of attention layer operations and memory operations before and after the All-to-All phase. Notably, the “Others” part of these methods has a smaller proportion compared to Megatron (Fig. 1(b)), because Megatron employs tensor parallelism for attention layers to handle memory consumption due to insufficient FSDP support, resulting in a higher proportion of time in “Others” due to TP’s communication overhead.

To further investigate the root cause, we analyze the maximum token count per device per layer across different methods, as illustrated in Fig. 10(b). The grey dashed line represents the token count for perfect balance. LAER-MoE consistently achieves minimal deviation from the ideal balance across all scenarios. In contrast, FlexMoE, which continuously adjusts previous expert layouts, may suffer from suboptimal adjustments when load changes, leading to suboptimal load balancing on e16k4. Meanwhile, LAER-MoE optimizes globally at each iteration, and with the e16k4 models increasing the number of experts per device, it provides more flexible optimization opportunities, achieving nearly perfect load balancing.

5.4 Planner Performance

We also analyze the efficiency of our planner algorithm. For lite routing, we measure the time consumed by each iteration’s related operations as a percentage of the total time, as shown in Tab. 3. The percentage is less than 0.1%, indicating that although the lite routing must execute synchronously

Table 3. Performance of lite routing.

Model	Lite Routing Time(ms)	Percentage of Total Time
Mixtral-8x7B e8k2	24.965	0.084%
Mixtral-8x7B e16k4	30.994	0.094%

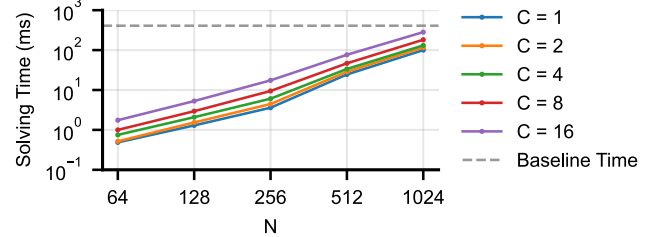


Figure 11. Performance of expert layout solver.

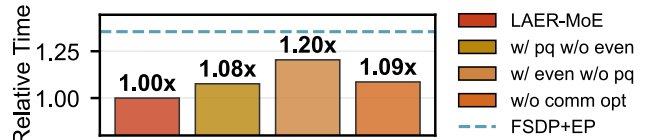


Figure 12. Ablation study on Mixtral-8x7B e8k2.

during training, it has almost no additional impact on end-to-end performance. The complexity of the replica allocation algorithm is $O(NC \log(NC))$, and the complexity of the expert placement algorithm is $O(N^2C)$, thus the complexity of the expert layout algorithm is $O(|\epsilon|N^2C)$. We fix $|\epsilon|$ to 2 (proportional and even allocation) and scale N and C to obtain the solving times shown in Fig. 11, where the grey dashed line represents the baseline time, i.e., which is the average total time consumed per transformer layer in Mixtral-8x7b-e8k2. As the cluster scale increases, the time per transformer layer exceeds the baseline time, yet even when scaled to 1024 GPUs, our algorithm remains highly efficient, consistently below the baseline time. Moreover, for larger C and N , since solving is layer-independent, we can parallelize solvers for different layers across multiple CPU processes to relax the real-time constraints. Thus, the planning will never become a bottleneck.

5.5 Ablation Study

To validate our expert layout solver and communication optimizations in LAER-MoE, we conduct ablation studies Mixtral-8x7b e8k2, as shown in Fig. 12. We compare LAER-MoE with incomplete solving algorithms that employ only a single expert replication scheme, where ‘pq’ denotes the priority queue proportional allocation scheme and ‘even’ indicates the even allocation scheme. It is evident that relying solely on one scheme cannot effectively handle all routing

distribution scenarios, while utilizing multiple replication schemes offers robust performance. For communication optimization, we compare LAER-MoE with a system lacking the communication optimizations in Fig. 5, revealing that without such optimizations, the overlap effect of communication is compromised, subsequently affecting end-to-end efficiency.

6 Related Work

Load Balancing in MoE Training. FasterMoE [11] broadcasts hot experts to all devices, introducing extra expert communication. SmartMoE [46] reassigns experts to co-locate hot and cold ones on the same device to alleviate load imbalance, but only changes expert locations without allowing replication. Prophet selectively replicates hot experts across nodes, yielding skewed parameter traffic proportional to replica count. FlexMoE [29] combines replacement and replication, dynamically tuning replica counts and locations of experts, but still cannot resolve the additional communication of expert parameters. Our newly proposed parallel paradigm is completely orthogonal to these methods and offers more flexible expert layout choices. Crucially, LAER-MoE supports per-iteration re-layout, enabling real-time adaptation even in scenarios with rapidly shifting expert hotspots. This capability ensures sustained training efficiency, offering a decisive advantage over prior approaches that are limited to infrequent, coarse-grained adjustments.

Communication and Computation optimizations. MegaBlocks [8] models expert GEMMs as sparse matrix multiplication and develops custom kernels. DeepSpeedMoE and MoESys [30, 45] reduce communication pairs via hierarchical optimizations. NetMoE [22] reorders sample placement to reduce inter-node communication. DeepEP [51] provides specialized All-to-All kernels. FasterMoE [11], Tutel [12], ScheMoE [35], MPMoE [50], and PipeMoE [34] chunk All-to-All and expert compute to overlap communication and computation. Comet [48] further fuses these into a single GPU kernel. HiDUp [36], Lancet [14], Lina [18], DeepSeek-V3 [5] refine the scheduling of communication and computation to achieve better overlap. All are orthogonal to our approach and can be composed with our work for higher throughput.

7 Discussion

Performance in Balanced Scenarios. As detailed in Sec. 3.1, our method’s communication volume is nearly identical to FSDP+EP. Consequently, in balanced expert load scenarios, the performance of LAER-MoE is comparable to FSDP+EP. However, we emphasize that LAER-MoE is architected primarily to address imbalanced scenarios. Our core objective is to decouple system efficiency from algorithmic constraints, providing researchers with the flexibility to explore algorithms with lower auxiliary loss weights (which potentially

yield better model quality) while maintaining high training throughput and system robustness.

Global Peak Memory Analysis. In Sec. 5.3, we report the relative maximum token count for different methods across various layers. This metric serves as an indirect proxy for per-layer activation memory usage (since memory consumption of activations is linear w.r.t. token counts). Since the heavy experts often differ from one layer to the next, FSDP+EP exhibits relatively balanced global peak memory across different ranks. Consequently, our method’s impact on the global peak memory is not significant. This does not conflict with our optimization goal: our method is designed to balance the computational load within each layer.

Scalability on Large-scale Clusters. While empirical experiments on large-scale clusters are limited by resource constraints, we provide a theoretical analysis to demonstrate the scalability of LAER-MoE. First, as cluster size increases, the reduced per-device memory footprint allows for larger micro-batch sizes, effectively compensating for a potential decrease in bandwidth (V_{comm}) and maintaining computation-communication overlap (Eq. 1). Second, in cross-rack scenarios where bandwidth is typically constrained, LAER-MoE is compatible with hybrid parallelism (e.g., Pipeline Parallelism), which can mitigate limited cross-rack bandwidth by confining All-to-All communication within racks to preserve training efficiency. Finally, we conducted simulations using real routing traces from Mixtral-8x7B-e8k2 training (detailed in Appendix D), which indicate that the speedup yielded by our re-layout algorithm remains stable as the cluster scales from 8 to 128 GPUs, demonstrating that our approach scales efficiently with cluster expansion.

8 Conclusion

We presented LAER-MoE, a novel system for distributed MoE training that addresses load balancing challenges. We proposed Fully Sharded Expert Parallelism (FSEP) paradigm, which enables flexible, in-training expert re-layout while removing re-layout communication overhead. We also designed an intelligent load balancing planner that dynamically co-optimizes token routing and expert layout, improving throughput without sacrificing model quality. Experiments show up to 1.69 \times acceleration over SOTA distributed systems, advancing efficient large-scale MoE training.

Acknowledgments

This work is supported by National Natural Science Foundation of China (U23B2048, 62402011), Fundamental and Interdisciplinary Disciplines Breakthrough Plan of the Ministry of Education of China (JYB2025XDXM108), ByteDance-PKU joint program, and High-performance Computing Platform of Peking University. Fangcheng Fu and Bin Cui are the corresponding authors.

References

[1] Suresh Bolusani, Mathieu Besançon, Ksenia Bestuzheva, Antonia Chmiela, João Dionísio, Tim Donkiewicz, Jasper van Doornmalen, Leon Eifler, Mohammed Ghannam, Ambros Gleixner, Christoph Graczyk, Katrin Halbig, Ivo Hettke, Alexander Hoen, Christopher Hoenig, Rolf van der Hulst, Dominik Kamp, Thorsten Koch, Kevin Kofler, Jurgen Lentz, Julian Manns, Gioni Mexi, Erik Mühmer, Marc E. Pfetsch, Franziska Schlösser, Felipe Serrano, Yuji Shinano, Mark Turner, Stefan Vigerske, Dieter Weninger, and Lixing Xu. 2024. *The SCIP Optimization Suite 9.0*. Technical Report. Optimization Online. <https://optimization-online.org/2024/02/the-scip-optimization-suite-9-0/>

[2] Tom B. Brown, Benjamin Mann, Nick Ryder, Melanie Subbiah, Jared Kaplan, Prafulla Dhariwal, Arvind Neelakantan, Pranav Shyam, Girish Sastry, Amanda Askell, Sandhini Agarwal, Ariel Herbert-Voss, Gretchen Krueger, Tom Henighan, Rewon Child, Aditya Ramesh, Daniel M. Ziegler, Jeffrey Wu, Clemens Winter, Christopher Hesse, Mark Chen, Eric Sigler, Mateusz Litwin, Scott Gray, Benjamin Chess, Jack Clark, Christopher Berner, Sam McCandlish, Alec Radford, Ilya Sutskever, and Dario Amodei. 2020. Language Models are Few-Shot Learners. In *Advances in Neural Information Processing Systems 33: Annual Conference on Neural Information Processing Systems 2020, NeurIPS 2020, December 6-12, 2020, virtual*, Hugo Larochelle, Marc'Aurelio Ranzato, Raia Hadsell, Maria-Florina Balcan, and Hsuan-Tien Lin (Eds.).

[3] Weilin Cai, Juyong Jiang, Fan Wang, Jing Tang, Sunghun Kim, and Jiayi Huang. 2025. A Survey on Mixture of Experts in Large Language Models. *IEEE Transactions on Knowledge and Data Engineering* (2025), 1–20.

[4] Aidan Clark, Diego de Las Casas, Aurelia Guy, Arthur Mensch, Michela Paganini, Jordan Hoffmann, Bogdan Damoc, Blake A. Hechtman, Trevor Cai, Sebastian Borgeaud, George van den Driessche, Eliza Rutherford, Tom Hennigan, Matthew J. Johnson, Albin Cassirer, Chris Jones, Elena Buchatskaya, David Budden, Laurent Sifre, Simon Osindero, Oriol Vinyals, Marc'Aurelio Ranzato, Jack W. Rae, Erich Elsen, Koray Kavukcuoglu, and Karen Simonyan. 2022. Unified Scaling Laws for Routed Language Models. In *International Conference on Machine Learning, ICML 2022, 17-23 July 2022, Baltimore, Maryland, USA (Proceedings of Machine Learning Research, Vol. 162)*, Kamalika Chaudhuri, Stefanie Jegelka, Le Song, Csaba Szepesvári, Gang Niu, and Sivan Sabato (Eds.). PMLR, 4057–4086.

[5] DeepSeek-AI, Aixin Liu, Bei Feng, Bing Xue, Bingxuan Wang, Bochao Wu, Chengda Lu, Chenggang Zhao, Chengqi Deng, Chenyu Zhang, Chong Ruan, Damai Dai, Daya Guo, Dejian Yang, Deli Chen, Dongjie Ji, Erhang Li, Fangyun Lin, Fucong Dai, Fuli Luo, Guangbo Hao, Guanting Chen, Guowei Li, H. Zhang, Han Bao, Hanwei Xu, Haocheng Wang, Haowei Zhang, Honghui Ding, Huajian Xin, Huazuo Gao, Hui Li, Hui Qu, J. L. Cai, Jian Liang, Jianzhong Guo, Jiaqi Ni, Jiashi Li, Jiawei Wang, Jin Chen, Jingchang Chen, Jingyang Yuan, Junjie Qiu, Junlong Li, Junxiao Song, Kai Dong, Kai Hu, Kaige Gao, Kang Guan, Kexin Huang, Kuai Yu, Lean Wang, Lecong Zhang, Lei Xu, Leyi Xia, Liang Zhao, Litong Wang, Liyue Zhang, Meng Li, Miaojun Wang, Mingchuan Zhang, Minghua Zhang, Minghui Tang, Mingming Li, Ning Tian, Panpan Huang, Peiyi Wang, Peng Zhang, Qiancheng Wang, Qihao Zhu, Qinyu Chen, Qiushi Du, R. J. Chen, R. L. Jin, Ruiqi Ge, Ruisong Zhang, Ruizhe Pan, Runji Wang, Runxin Xu, Ruoyu Zhang, Ruyi Chen, S. S. Li, Shanghao Lu, Shangyan Zhou, Shanhuan Chen, Shaoqing Wu, Shengfeng Ye, Shengfeng Ye, Shirong Ma, Shiyu Wang, Shuang Zhou, Shuiping Yu, Shunfeng Zhou, Shuting Pan, T. Wang, Tao Yun, Tian Pei, Tianyu Sun, W. L. Xiao, and Wangding Zeng. 2024. DeepSeek-V3 Technical Report. *CoRR* abs/2412.19437 (2024).

[6] Abhimanyu Dubey, Abhinav Jauhri, Abhinav Pandey, Abhishek Kadian, Ahmad Al-Dahle, Aiesha Letman, Akhil Mathur, Alan Schellen, Amy Yang, Angela Fan, Anirudh Goyal, Anthony Hartshorn, Aobo Yang, Archi Mitra, Archie Sravankumar, Artem Korenev, Arthur Hinsvark, Arun Rao, Aston Zhang, Aurélien Rodriguez, Austen Gregerson, Ava Spataru, Baptiste Rozière, Bethany Biron, Binh Tang, Bobbie Chern, Charlotte Caucheteux, Chaya Nayak, Chloe Bi, Chris Marra, Chris McConnell, Christian Keller, Christophe Touret, Chongyang Wu, Corinne Wong, Cristian Canton Ferrer, Cyrus Nikolaidis, Damien Allonsius, Daniel Song, Danielle Pintz, Danny Livshits, David Esibou, Dhruv Choudhary, Dhruv Mahajan, Diego Garcia-Olano, Diego Perino, Dieuwke Hupkes, Egor Lakomkin, Ehab AlBadawy, Elina Lobanova, Emily Dinan, Eric Michael Smith, Filip Radenovic, Frank Zhang, Gabriel Synnaeve, Gabrielle Lee, Georgia Lewis Anderson, Graeme Nail, Grégoire Mialon, Guan Pang, Guillem Cucurell, Hailey Nguyen, Hannah Korevaar, Hu Xu, Hugo Touvron, Iliyan Zarov, Imanol Arrieta Ibarra, Isabel M. Kloumann, Ishan Misra, Ivan Evtimov, Jade Copet, Jaewon Lee, Jan Geffert, Jana Vrane, Jason Park, Jay Mahadeokar, Jeet Shah, Jelmer van der Linde, Jennifer Billock, Jenny Hong, Jinya Lee, Jeremy Fu, Jianfeng Chi, Jianyu Huang, Jiawen Liu, Jie Wang, Jiecao Yu, Joanna Bitton, Joe Spisak, Jongsoo Park, Joseph Rocca, Joshua Johnstun, Joshua Saxe, Junteng Jia, Kalyan Vasudan Alwala, Kartikeya Upasani, Kate Plawiak, Ke Li, Kenneth Heafield, Kevin Stone, and et al. 2024. The Llama 3 Herd of Models. *CoRR* abs/2407.21783 (2024).

[7] William Fedus, Barret Zoph, and Noam Shazeer. 2022. Switch Transformers: Scaling to Trillion Parameter Models with Simple and Efficient Sparsity. *J. Mach. Learn. Res.* 23 (2022), 120:1–120:39.

[8] Trevor Gale, Deepak Narayanan, Cliff Young, and Matei Zaharia. 2023. MegaBlocks: Efficient Sparse Training with Mixture-of-Experts. In *Proceedings of the Sixth Conference on Machine Learning and Systems, MLSys 2023, Miami, FL, USA, June 4-8, 2023*, Dawn Song, Michael Carbin, and Tianqi Chen (Eds.). mlsys.org.

[9] Amir Gholami. 2021. AI and Memory Wall. <https://medium.com/riselab/ai-and-memory-wall-2cb4265cb0b8>. blog.

[10] Lei Guan, Dong-Sheng Li, Jiye Liang, Wen-Jian Wang, Ke-shi Ge, and Xicheng Lu. 2024. Advances of Pipeline Model Parallelism for Deep Learning Training: An Overview. *J. Comput. Sci. Technol.* 39, 3 (2024), 567–584.

[11] Jiaao He, Jidong Zhai, Tiago Antunes, Haojie Wang, Fuwen Luo, Shangfeng Shi, and Qin Li. 2022. FasterMoE: modeling and optimizing training of large-scale dynamic pre-trained models. In *PPoPP '22: 27th ACM SIGPLAN Symposium on Principles and Practice of Parallel Programming, Seoul, Republic of Korea, April 2 - 6, 2022*, Jaejin Lee, Kunal Agrawal, and Michael F. Spear (Eds.). ACM, 120–134.

[12] Changho Hwang, Wei Cui, Yifan Xiong, Ziyue Yang, Ze Liu, Han Hu, Zilong Wang, Rafael Salas, Jithin Jose, Prabhat Ram, HoYuen Chau, Peng Cheng, Fan Yang, Mao Yang, and Yongqiang Xiong. 2023. Tutel: Adaptive Mixture-of-Experts at Scale. In *Proceedings of the Sixth Conference on Machine Learning and Systems, MLSys 2023, Miami, FL, USA, June 4-8, 2023*, Dawn Song, Michael Carbin, and Tianqi Chen (Eds.). mlsys.org.

[13] Albert Q. Jiang, Alexandre Sablayrolles, Antoine Roux, Arthur Mensch, Blanche Savary, Chris Bamford, Devendra Singh Chaplot, Diego de Las Casas, Emma Bou Hanna, Florian Bressand, Gianna Lengyel, Guillaume Bour, Guillaume Lample, Lélio Renard Lavaud, Lucile Saulnier, Marie-Anne Lachaux, Pierre Stock, Sandeep Subramanian, Sophia Yang, Szymon Antoniak, Teven Le Scao, Théophile Gervet, Thibaut Lavril, Thomas Wang, Timothée Lacroix, and William El Sayed. 2024. Mixtral of Experts. *CoRR* abs/2401.04088 (2024).

[14] Chenyu Jiang, Ye Tian, Zhen Jia, Shuai Zheng, Chuan Wu, and Yida Wang. 2024. Lancet: Accelerating Mixture-of-Experts Training via Whole Graph Computation-Communication Overlapping. In *Proceedings of the Seventh Annual Conference on Machine Learning and Systems, MLSys 2024, Santa Clara, CA, USA, May 13-16, 2024*, Phillip B. Gibbons, Gennady Pekhimenko, and Christopher De Sa (Eds.). mlsys.org.

[15] Chao Jin, Ziheng Jiang, Zhihao Bai, Zheng Zhong, Juncai Liu, Xiang Li, Ningxin Zheng, Xi Wang, Cong Xie, Qi Huang, Wen Heng, Yiyuan Ma, Wenlei Bao, Size Zheng, Yanghua Peng, Haibin Lin, Xuanzhe Liu, Xin

Jin, and Xin Liu. 2025. MegaScale-MoE: Large-Scale Communication-Efficient Training of Mixture-of-Experts Models in Production. *CoRR* abs/2505.11432 (2025).

[16] Dmitry Lepikhin, HyoukJoong Lee, Yuanzhong Xu, Dehao Chen, Orhan Firat, Yaping Huang, Maxim Krikun, Noam Shazeer, and Zhipeng Chen. 2021. GShard: Scaling Giant Models with Conditional Computation and Automatic Sharding. In *9th International Conference on Learning Representations, ICLR 2021, Virtual Event, Austria, May 3-7, 2021*. OpenReview.net.

[17] Mike Lewis, Shruti Bhosale, Tim Dettmers, Naman Goyal, and Luke Zettlemoyer. 2021. BASE Layers: Simplifying Training of Large, Sparse Models. In *Proceedings of the 38th International Conference on Machine Learning, ICML 2021, 18-24 July 2021, Virtual Event (Proceedings of Machine Learning Research, Vol. 139)*, Marina Meila and Tong Zhang (Eds.). PMLR, 6265–6274.

[18] Jiamin Li, Yimin Jiang, Yibo Zhu, Cong Wang, and Hong Xu. 2023. Accelerating Distributed MoE Training and Inference with Lina. In *Proceedings of the 2023 USENIX Annual Technical Conference, USENIX ATC 2023, Boston, MA, USA, July 10-12, 2023*, Julia Lawall and Dan Williams (Eds.). USENIX Association, 945–959.

[19] Juntao Li, Zecheng Tang, Yuyang Ding, Pinzheng Wang, Pei Guo, Wangjie You, Dan Qiao, Chenyu Wang, Wenliang Chen, Guohong Fu, Qiaoming Zhu, Guodong Zhou, and Min Zhang. 2025. OpenBA: an open-sourced 15B bilingual asymmetric Seq2Seq model pre-trained from scratch. *Sci. China Inf. Sci.* 68, 9 (2025).

[20] Shen Li, Yanli Zhao, Rohan Varma, Omkar Salpekar, Pieter Noordhuis, Teng Li, Adam Paszke, Jeff Smith, Brian Vaughan, Pritam Damania, and Soumith Chintala. 2020. PyTorch Distributed: Experiences on Accelerating Data Parallel Training. *Proc. VLDB Endow.* 13, 12 (2020), 3005–3018.

[21] Dennis Liu, Zijie Yan, Xin Yao, Tong Liu, Vijay Korthikanti, Evan Wu, Shiqing Fan, Gao Deng, Hongxiao Bai, Jianbin Chang, Ashwath Aithal, Michael Andersch, Mohammad Shoeybi, Jiajie Yao, Chandler Zhou, David Wu, Xipeng Li, and June Yang. 2025. MoE Parallel Folding: Heterogeneous Parallelism Mappings for Efficient Large-Scale MoE Model Training with Megatron Core. *CoRR* abs/2504.14960 (2025).

[22] Xinyi Liu, Yujie Wang, Fangcheng Fu, Xupeng Miao, Shenhan Zhu, Xiaonan Nie, and Bin Cui. 2025. NetMoE: Accelerating MoE Training through Dynamic Sample Placement. In *The Thirteenth International Conference on Learning Representations, ICLR 2025, Singapore, April 24-28, 2025*. OpenReview.net.

[23] Xinyi Liu, Yujie Wang, Shenhan Zhu, Fangcheng Fu, Qingshuo Liu, Guangming Lin, and Bin Cui. 2025. Galvatron: An Automatic Distributed System for Efficient Foundation Model Training. *CoRR* abs/2504.21411 (2025).

[24] Zixuan Ma, Jiaao He, Jiezhong Qiu, Huanqi Cao, Yuanwei Wang, Zhenbo Sun, Liyan Zheng, Haojie Wang, Shizhi Tang, Tianyu Zheng, Junyang Lin, Guanyu Feng, Zeqiang Huang, Jie Gao, Aohan Zeng, Jianwei Zhang, Runxin Zhong, Tianhui Shi, Sha Liu, Weimin Zheng, Jie Tang, Hongxia Yang, Xin Liu, Jidong Zhai, and Wenguang Chen. 2022. BaGuaLu: targeting brain scale pretrained models with over 37 million cores. In *PPoPP '22: 27th ACM SIGPLAN Symposium on Principles and Practice of Parallel Programming, Seoul, Republic of Korea, April 2 - 6, 2022*, Jaejin Lee, Kunal Agrawal, and Michael F. Spear (Eds.). ACM, 192–204.

[25] Xupeng Miao, Yujie Wang, Youhe Jiang, Chunan Shi, Xiaonan Nie, Hailin Zhang, and Bin Cui. 2022. Galvatron: Efficient Transformer Training over Multiple GPUs Using Automatic Parallelism. *Proc. VLDB Endow.* 16, 3 (2022), 470–479.

[26] Deepak Narayanan, Aaron Harlap, Amar Phanishayee, Vivek Seshadri, Nikhil R. Devanur, Gregory R. Ganger, Phillip B. Gibbons, and Matei Zaharia. 2019. PipeDream: generalized pipeline parallelism for DNN training. In *Proceedings of the 27th ACM Symposium on Operating Systems Principles, SOSP 2019, Huntsville, ON, Canada, October 27-30, 2019*, Tim Brecht and Carey Williamson (Eds.). ACM, 1–15.

[27] Deepak Narayanan, Amar Phanishayee, Kaiyu Shi, Xie Chen, and Matei Zaharia. 2021. Memory-Efficient Pipeline-Parallel DNN Training. In *Proceedings of the 38th International Conference on Machine Learning, ICML 2021, 18-24 July 2021, Virtual Event (Proceedings of Machine Learning Research, Vol. 139)*, Marina Meila and Tong Zhang (Eds.). PMLR, 7937–7947.

[28] Deepak Narayanan, Mohammad Shoeybi, Jared Casper, Patrick LeGresley, Mostofa Patwary, Vijay Korthikanti, Dmitri Vainbrand, Prethvi Kashinkunti, Julie Bernauer, Bryan Catanzaro, Amar Phanishayee, and Matei Zaharia. 2021. Efficient large-scale language model training on GPU clusters using megatron-LM. In *International Conference for High Performance Computing, Networking, Storage and Analysis, SC 2021, St. Louis, Missouri, USA, November 14-19, 2021*, Bronis R. de Supinski, Mary W. Hall, and Todd Gamblin (Eds.). ACM, 58.

[29] Xiaonan Nie, Xupeng Miao, Zilong Wang, Zichao Yang, Jilong Xue, Lingxiao Ma, Gang Cao, and Bin Cui. 2023. FlexMoE: Scaling Large-scale Sparse Pre-trained Model Training via Dynamic Device Placement. *Proc. ACM Manag. Data* 1, 1 (2023), 110:1–110:19.

[30] Samyam Rajbhandari, Conglong Li, Zhewei Yao, Minjia Zhang, Reza Yazdani Aminabadi, Ammar Ahmad Awan, Jeff Rasley, and Yuxiong He. 2022. DeepSpeed-MoE: Advancing Mixture-of-Experts Inference and Training to Power Next-Generation AI Scale. In *International Conference on Machine Learning, ICML 2022, 17-23 July 2022, Baltimore, Maryland, USA (Proceedings of Machine Learning Research, Vol. 162)*, Kamalika Chaudhuri, Stefanie Jegelka, Le Song, Csaba Szepesvári, Gang Niu, and Sivan Sabato (Eds.). PMLR, 18332–18346.

[31] Samyam Rajbhandari, Jeff Rasley, Olatunji Ruwase, and Yuxiong He. 2020. ZeRO: memory optimizations toward training trillion parameter models. In *Proceedings of the International Conference for High Performance Computing, Networking, Storage and Analysis, SC 2020, Virtual Event / Atlanta, Georgia, USA, November 9-19, 2020*, Christine Cuicchi, Irene Qualters, and William T. Kramer (Eds.). IEEE/ACM, 20.

[32] Stephen Roller, Sainbayar Sukhbaatar, Arthur Szlam, and Jason Weston. 2021. Hash Layers For Large Sparse Models. In *Advances in Neural Information Processing Systems 34: Annual Conference on Neural Information Processing Systems 2021, NeurIPS 2021, December 6-14, 2021, virtual*, Marc'Aurelio Ranzato, Alina Beygelzimer, Yann N. Dauphin, Percy Liang, and Jennifer Wortman Vaughan (Eds.). 17555–17566.

[33] Noam Shazeer, Azalia Mirhoseini, Krzysztof Maziarz, Andy Davis, Quoc V. Le, Geoffrey E. Hinton, and Jeff Dean. 2017. Outrageously Large Neural Networks: The Sparsely-Gated Mixture-of-Experts Layer. In *5th International Conference on Learning Representations, ICLR 2017, Toulon, France, April 24-26, 2017, Conference Track Proceedings*. OpenReview.net.

[34] Shaohuai Shi, Xinglin Pan, Xiaowen Chu, and Bo Li. 2023. PipeMoE: Accelerating Mixture-of-Experts through Adaptive Pipelining. In *IEEE INFOCOM 2023 - IEEE Conference on Computer Communications, New York City, NY, USA, May 17-20, 2023*. IEEE, 1–10.

[35] Shaohuai Shi, Xinglin Pan, Qiang Wang, Chengjian Liu, Xiaozhe Ren, Zhongzhe Hu, Yu Yang, Bo Li, and Xiaowen Chu. 2024. ScheMoE: An Extensible Mixture-of-Experts Distributed Training System with Tasks Scheduling. In *Proceedings of the Nineteenth European Conference on Computer Systems, EuroSys 2024, Athens, Greece, April 22-25, 2024*. ACM, 236–249.

[36] Athinagoras Skiadopoulos, Mark Zhao, Swapnil Gandhi, Thomas Norrie, Shrijeet Mukherjee, and Christos Kozyrakis. 2025. Accelerating Mixture-of-Experts Training with Adaptive Expert Replication. *CoRR* abs/2504.19925 (2025).

[37] Yehui Tang, Yichun Yin, Yaoyuan Wang, Hang Zhou, Wei Guo, Zhiguo Zhang, Miao Rang, Fangcheng Liu, Naifu Zhang, Binghan Li, Yonghan Dong, Xiaojun Meng, Yasheng Wang, Dong Li, Yin Li, Dandan Tu, Can Chen, Youliang Yan, Fisher Yu, Ruiming Tang, Yunhe Wang, Botian Huang, Bo Wang, Boxiao Liu, Changzheng Zhang, Da Kuang,

Fei Liu, Gang Huang, Jiansheng Wei, Jiarui Qin, Jie Ran, Jinpeng Li, Jun Zhao, Liang Dai, Lin Li, Liqun Deng, Peifeng Qin, Pengyuan Zeng, Qiang Gu, Shaohua Tang, Shengjun Cheng, Tao Gao, Tao Yu, Tianshu Li, Tianyu Bi, Wei He, Weikai Mao, Wenyong Huang, Wulong Liu, Xiabing Li, Xianzhi Yu, Xueyu Wu, Xu He, Yangkai Du, Yan Xu, Ye Tian, Yimeng Wu, Yongbing Huang, Yong Tian, Yong Zhu, Yue Li, Yufei Wang, Yuhang Gai, Yujun Li, Yu Luo, Yunsheng Ni, Yusen Sun, Zelin Chen, Zhe Liu, Zhipeng Tu, Zilin Ding, and Zongyuan Zhan. 2025. Pangu Ultra MoE: How to Train Your Big MoE on Ascend NPUs. *CoRR* abs/2505.04519 (2025).

[38] Hugo Touvron, Louis Martin, Kevin Stone, Peter Albert, Amjad Almehairi, Yasmine Babaei, Nikolay Bashlykov, Soumya Batra, Prajwal Bhargava, Shruti Bhosale, Dan Bikel, Lukas Blecher, Cristian Canton-Ferrer, Moya Chen, Guillem Cucurull, David Esiobu, Jude Fernandes, Jeremy Fu, Wenyin Fu, Brian Fuller, Cynthia Gao, Vedanuj Goswami, Naman Goyal, Anthony Hartshorn, Saghaf Hosseini, Rui Hou, Hakan Inan, Marcin Kardas, Viktor Kerkez, Madian Khabsa, Isabel Kloumann, Artem Korenev, Punit Singh Koura, Marie-Anne Lachaux, Thibaut Lavril, Jenya Lee, Diana Liskovich, Yinghai Lu, Yuning Mao, Xavier Martinet, Todor Mihaylov, Pushkar Mishra, Igor Molybog, Yixin Nie, Andrew Poulton, Jeremy Reizenstein, Rashi Rungta, Kalyan Saladi, Alan Schelten, Ruan Silva, Eric Michael Smith, Ranjan Subramanian, Xiaoqing Ellen Tan, Binh Tang, Ross Taylor, Adina Williams, Jian Xiang Kuan, Puxin Xu, Zheng Yan, Iliyan Zarov, Yuchen Zhang, Angela Fan, Melanie Kambadur, Sharan Narang, Aurélien Rodriguez, Robert Stojnic, Sergey Edunov, and Thomas Scialom. 2023. Llama 2: Open Foundation and Fine-Tuned Chat Models. *CoRR* abs/2307.09288 (2023).

[39] Ashish Vaswani, Noam Shazeer, Niki Parmar, Jakob Uszkoreit, Llion Jones, Aidan N. Gomez, Łukasz Kaiser, and Illia Polosukhin. 2017. Attention is All you Need. In *Advances in Neural Information Processing Systems 30: Annual Conference on Neural Information Processing Systems 2017, December 4-9, 2017, Long Beach, CA, USA*, Isabelle Guyon, Ulrike von Luxburg, Samy Bengio, Hanna M. Wallach, Rob Fergus, S. V. N. Vishwanathan, and Roman Garnett (Eds.). 5998–6008.

[40] Wei Wang, Zhiqian Lai, Shengwei Li, Weijie Liu, Keshi Ge, Yujie Liu, Ao Shen, and Dongsheng Li. 2023. Prophet: Fine-grained Load Balancing for Parallel Training of Large-scale MoE Models. In *IEEE International Conference on Cluster Computing, CLUSTER 2023, Santa Fe, NM, USA, October 31 - Nov. 3, 2023*. IEEE, 82–94.

[41] Yujie Wang, Youhe Jiang, Xupeng Miao, Fangcheng Fu, Shenhan Zhu, Xiaonan Nie, Yaofeng Tu, and Bin Cui. 2024. Improving Automatic Parallel Training via Balanced Memory Workload Optimization. *IEEE Trans. Knowl. Data Eng.* 36, 8 (2024), 3906–3920.

[42] Weikai Xu, Chengrui Huang, Shen Gao, and Shuo Shang. 2025. LLM-Based Agents for Tool Learning: A Survey. *Data Sci. Eng.* 10, 4 (2025), 533–563.

[43] An Yang, Anfeng Li, Baosong Yang, Beichen Zhang, Binyuan Hui, Bo Zheng, Bowen Yu, Chang Gao, Chengan Huang, Chenxu Lv, Chujie Zheng, Dayiheng Liu, Fan Zhou, Fei Huang, Feng Hu, Hao Ge, Haoran Wei, Huan Lin, Jialong Tang, Jian Yang, Jianhong Tu, Jianwei Zhang, Jianxin Yang, Jiaxi Yang, Jing Zhou, Jingren Zhou, Junyang Lin, Kai Dang, Keqin Bao, Kexin Yang, Le Yu, Lianghao Deng, Mei Li, Mingfeng Xue, Mingze Li, Pei Zhang, Peng Wang, Qin Zhu, Rui Men, Ruize Gao, Shixuan Liu, Shuang Luo, Tianhao Li, Tianyi Tang, Wenbiao Yin, Xingzhang Ren, Xinyu Wang, Xinyu Zhang, Xuancheng Ren, Yang Fan, Yang Su, Yichang Zhang, Yinger Zhang, Yu Wan, Yuqiong Liu, Zekun Wang, Zeyu Cui, Zhenru Zhang, Zhipeng Zhou, and Zihan Qiu. 2025. Qwen3 Technical Report. *CoRR* abs/2505.09388 (2025).

[44] An Yang, Baosong Yang, Beichen Zhang, Binyuan Hui, Bo Zheng, Bowen Yu, Chengyuan Li, Dayiheng Liu, Fei Huang, Haoran Wei, Huan Lin, Jian Yang, Jianhong Tu, Jianwei Zhang, Jianxin Yang, Jiaxi Yang, Jingren Zhou, Junyang Lin, Kai Dang, Keming Lu, Keqin Bao, Kexin Yang, Le Yu, Mei Li, Mingfeng Xue, Pei Zhang, Qin Zhu, Rui Men, Runji Lin, Tianhao Li, Tingyu Xia, Xingzhang Ren, Xuancheng Ren, Yang Fan, Yang Su, Yichang Zhang, Yu Wan, Yuqiong Liu, Zeyu Cui, Zhenru Zhang, and Zihan Qiu. 2024. Qwen2.5 Technical Report. *CoRR* abs/2412.15115 (2024).

[45] Dianhai Yu, Liang Shen, Hongxiang Hao, Weibao Gong, HuaChao Wu, Jiang Bian, Lirong Dai, and Haoyi Xiong. 2024. MoESys: A Distributed and Efficient Mixture-of-Experts Training and Inference System for Internet Services. *IEEE Trans. Serv. Comput.* 17, 5 (2024), 2626–2639.

[46] Mingshu Zhai, Jiaao He, Zixuan Ma, Zan Zong, Runjing Zhang, and Jidong Zhai. 2023. SmartMoE: Efficiently Training Sparsely-Activated Models through Combining Offline and Online Parallelization. In *Proceedings of the 2023 USENIX Annual Technical Conference, USENIX ATC 2023, Boston, MA, USA, July 10-12, 2023*, Julia Lawall and Dan Williams (Eds.). USENIX Association, 961–975.

[47] Huangzhao Zhang, Kechi Zhang, Zhuo Li, Jia Li, Jia Li, Yongmin Li, Yunfei Zhao, Yuqi Zhu, Fang Liu, Ge Li, et al. 2024. Deep learning for code generation: a survey. *Sci. China Inf. Sci.* 67, 9 (2024).

[48] Shulai Zhang, Ningxin Zheng, Haibin Lin, Ziheng Jiang, Wenlei Bao, Chengquan Jiang, Qi Hou, Weihao Cui, Size Zheng, Li-Wen Chang, Quan Chen, and Xin Liu. 2025. Comet: Fine-grained Computation-communication Overlapping for Mixture-of-Experts. *CoRR* abs/2502.19811 (2025).

[49] Zhenxing Zhang, Yuanbo Wen, Han-Qi Lyu, Chang Liu, Rui Zhang, Xia-Qing Li, Chao Wang, Zidong Du, Qi Guo, Ling Li, Xue-Hai Zhou, and Yun-Ji Chen. 2025. AI Computing Systems for Large Language Models Training. *J. Comput. Sci. Technol.* 40, 1 (2025), 6–41.

[50] Zheng Zhang, Yaqi Xia, Hulin Wang, Donglin Yang, Chuang Hu, Xiaobo Zhou, and Dazhao Cheng. 2024. MPMoE: Memory Efficient MoE for Pre-Trained Models With Adaptive Pipeline Parallelism. *IEEE Trans. Parallel Distributed Syst.* 35, 6 (2024), 843–856.

[51] Chenggang Zhao, Shangyan Zhou, Liyue Zhang, Chengqi Deng, Zhean Xu, Yuxuan Liu, Kuai Yu, Jia Shi Li, and Liang Zhao. 2025. DeepEP: an efficient expert-parallel communication library. <https://github.com/deepseek-ai/DeepEP>.

[52] Wayne Xin Zhao, Kun Zhou, Junyi Li, Tianyi Tang, Xiaolei Wang, Yupeng Hou, Yingqian Min, Beichen Zhang, Junjie Zhang, Zican Dong, Yifan Du, Chen Yang, Yushuo Chen, Zhipeng Chen, Jinhao Jiang, Ruiyang Ren, Yifan Li, Xinyu Tang, Zikang Liu, Peiyu Liu, Jian-Yun Nie, and Ji-Rong Wen. 2023. A Survey of Large Language Models. *CoRR* abs/2303.18223 (2023).

[53] Yanli Zhao, Andrew Gu, Rohan Varma, Liang Luo, Chien-Chin Huang, Min Xu, Less Wright, Hamid Shojanazeri, Myle Ott, Sam Shleifer, Alban Desmaison, Can Balioglu, Pritam Damania, Bernard Nguyen, Geeta Chauhan, Yuchen Hao, Ajit Mathews, and Shen Li. 2023. PyTorch FSDP: Experiences on Scaling Fully Shared Data Parallel. *Proc. VLDB Endow.* 16, 12 (2023), 3848–3860.

[54] Xuanhe Zhou, Zhaoyan Sun, and Guoliang Li. 2024. DB-GPT: Large Language Model Meets Database. *Data Sci. Eng.* 9, 1 (2024), 102–111.

[55] Yanqi Zhou, Tao Lei, Hanxiao Liu, Nan Du, Yanping Huang, Vincent Y. Zhao, Andrew M. Dai, Zifeng Chen, Quoc V. Le, and James Laudon. 2022. Mixture-of-Experts with Expert Choice Routing. In *Advances in Neural Information Processing Systems 35: Annual Conference on Neural Information Processing Systems 2022, NeurIPS 2022, New Orleans, LA, USA, November 28 - December 9, 2022*, Sanmi Koyejo, S. Mohamed, A. Agarwal, Danielle Belgrave, K. Cho, and A. Oh (Eds.).

[56] Tong Zhu, Xiaoye Qu, Daize Dong, Jiacheng Ruan, Jingqi Tong, Conghui He, and Yu Cheng. 2024. LLaMA-MoE: Building Mixture-of-Experts from LLaMA with Continual Pre-Training. In *Proceedings of the 2024 Conference on Empirical Methods in Natural Language Processing, EMNLP 2024, Miami, FL, USA, November 12-16, 2024*, Yaser Al-Onaizan, Mohit Bansal, and Yun-Nung Chen (Eds.). Association for Computational Linguistics, 15913–15923.

A Artifact Appendix

A.1 Abstract

This artifact includes codes and scripts for reproducing all experiments in the paper. The artifact contains the implementation of LAER-MoE along with baseline implementations (Megatron-LM, FSDP-EP, FLEX-MoE), training scripts for various MoE models (Mixtral-8x7B, Mixtral-8x22B, Qwen-8x7B), and evaluation scripts to reproduce all experimental results including end-to-end performance (Figure 8), convergence study (Figure 9), case study (Figure 10), planner performance (Figure 11), and ablation study (Figure 12).

A.2 Artifact check-list (meta-information)

- **Program:** Python, PyTorch, CUDA
- **Compilation:** NVCC 12.1, CMake \geq 3.21
- **Model:** Mixtral-8x7B, Mixtral-8x22B, Qwen-8x7B with different expert configurations (e8k2, e16k4)
- **Data set:** WikiText-103, C4
- **Run-time environment:** Python 3.9.2, CUDA 12.1, NCCL 2.18.1
- **Hardware:** 4-node GPU cluster, each node with 8 NVIDIA A100 80GB GPUs, NVLink (300 GB/s intra-node), Infiniband (800 Gbps inter-node)
- **Execution:** Distributed training using `torch.distributed.launch`
- **Metrics:** End-to-end performance (Training throughput (tokens/s))
- **Output:** End-to-end training throughput, loss curves, and figures.
- **Experiments:** End-to-end, convergence study, case study, planner performance, ablation study
- **How much disk space required (approximately)?:** 200 GB for per model checkpoints, 2TB in total.
- **How much time is needed to prepare workflow (approximately)?:** 2-4 hours for environment setup and installation.
- **How much time is needed to complete experiments (approximately)?:** 0.5-1 hour per-configuration for most experiments, 10 hours per-configuration for each convergence study.
- **Publicly available?:** Yes (Anonymized link provided for review)
- **Code licenses (if publicly available)?:** Apache 2.0
- **Workflow automation framework used?:** Bash scripts
- **Archived (provide DOI)?:** 10.5281/zenodo.18298795

A.3 Description

A.3.1 How to access. The artifact is available on GitHub repository (<https://github.com/Fizzmy/LAER-MoE-AE>) and Zenodo (<https://doi.org/10.5281/zenodo.18298795>), including installation instructions, experiment workflow, and expected results.

A.3.2 Hardware dependencies. We conduct our experiments on a 4-node GPU cluster, with each node containing 8 NVIDIA A100 80GB GPUs. Within nodes, GPUs are connected via NVLink with peak unidirectional communication

bandwidth of 300 GB/s intra-node. Nodes are interconnected via Infiniband with 800 Gbps bandwidth inter-node.

A.3.3 Software dependencies. The following software dependencies are required:

- Python 3.9.2
- CUDA 12.1
- PyTorch 2.1.0 (cu121)
- Flash-Attention v2.5.8
- Apex (commit 312acb4)
- Transformer-Engine (commit 7f2afaa, for baseline only)
- CMake \geq 3.21 (for baseline only)
- Additional Python packages: packaging, ninja, bsutil, pybind11, einops

A.3.4 Data sets. We use two datasets for evaluation:

- WikiText-103: A language modeling dataset containing over 100 million tokens from Wikipedia articles
- C4: A colossal, cleaned version of Common Crawl's web crawl corpus

The datasets are preprocessed using the Mixtral tokenizer.

A.3.5 Models. We evaluate on the following MoE model configurations:

- Mixtral-8x7B: e8k2 and e16k4 configurations
- Mixtral-8x22B: e8k2 and e16k4 configurations
- Qwen-8x7B: e8k2 and e16k4 configurations

where e8k2 means 8 experts with top-2 routing, and e16k4 means 16 experts with top-4 routing.

A.4 Installation

Users need to create a virtual environment and install PyTorch, Flash-Attention, Apex, and Transformer-Engine. Please refer to `README.md` for detailed instructions. To install LAER-MoE, use the following commands:

```
cd LAER-MoE
pip install -r requirements.txt
pip install -e . --no-build-isolation
```

A.5 Experiment workflow

All experiments should be conducted from the `./LAER-MoE` directory.

A.5.1 Prepare Datasets and Checkpoints. For datasets preparation, users should preprocess the datasets using Mixtral tokenizer. Please refer to `README.md` for detailed preprocessing instructions.

For checkpoints preparation, users should generate checkpoints for each model configuration before running experiments. Please refer to `LAER-MoE/README.md` for detailed instructions on checkpoint generation.

A.5.2 Performing Experiments. We provide shell scripts to perform experiments for each figure in the paper. All scripts are located in LAER-MoE/scripts_ae/.

End-to-End Performance (Figure 8): e2e.sh will start the end-to-end evaluation in §5.2. Users can run the following command for each configuration:

```
bash scripts_ae/e2e.sh <approach> <model_name> <aux_loss> <dataset>
```

where:

- <approach>: LAER, FLEX, FSDP, or megatron
- <model_name>: one of
 - mixtral-8x7b-e8k2
 - mixtral-8x7b-e16k4
 - mixtral-8x22b-e8k2
 - mixtral-8x22b-e16k4
 - qwen-8x7b-e8k2
 - qwen-8x7b-e16k4
- <aux_loss>: 0.0 or 1e-4
- <dataset>: wikitext or C4

We also provide a script to run the end-to-end evaluation for all the models and all the approaches. Users can run the following command:

```
bash scripts_ae/e2e_all.sh
```

Users can modify the e2e_all.sh script to run the end-to-end evaluation for different models and different approaches.

Convergence Study (Figure 9): convergence.sh will start the convergence study in §5.2. Users can run the following command:

```
bash scripts_ae/convergence.sh <approach> <aux_loss> <iter>
```

where (<approach>, <aux_loss>) can be (LAER, 1e-4), (Megatron, 1e-2), or (Megatron, 1e-4). Set <iter> to 3000 for full results or 1500 for faster artifact evaluation.

Case Study (Figure 10): We provide two scripts to perform case study for breakdown and maximum token counts.

Breakdown (Figure 10a): breakdown.sh will start the breakdown study in §5.3. Users can run the following command:

```
bash scripts_ae/breakdown.sh <approach> <model_name>
```

Maximum token counts (Figure 10b): token_counts.sh will start the maximum token counts study in §5.3. Users can run the following command:

```
bash scripts_ae/token_counts.sh <approach> <model_name>
```

where <approach> is LAER, FLEX, or FSDP, and <model_name> is mixtral-8x7b-e8k2 or mixtral-8x7b-e16k4.

Planner Performance (Figure 11): planner.sh will start the planner performance study in §5.4. Users can run the following command:

```
bash scripts_ae/planner.sh <N> <C>
```

where <N> is the number of devices and <C> is the capacity of experts per device. To get average time for all (N, C) pairs, run without arguments:

```
bash scripts_ae/planner.sh
```

Ablation Study (Figure 12): ablation.sh will start the ablation study in §5.5. Users can run the following command:

```
bash scripts_ae/ablation.sh <approach>
```

where <approach> is LAER, no_even, no_pq, no_comm_opt, or FSDP.

A.5.3 Plotting Figures. To generate figures from experimental results:

```
bash scripts_ae/plot.sh <figure_id> <type>
```

where <figure_id> is 8, 9, 10a, 10b, 11, or 12, and <type> is default (use paper data) or new (use newly generated experimental results).

A.6 Evaluation and expected results

The absolute performance numbers may vary across different hardware and network configurations. However, we expect that the relative performance trends shown in Figures 8–12 should be reproducible, with the average speedup ratios remaining comparable to those reported in the paper.

A.7 Experiment customization

Users can customize the evaluation scripts to test the system performance on other workloads with different model architectures, datasets, or training parameters. Please refer to LAER-MoE/README.md for detailed instructions on customization options and parameters.

A.8 Notes

- The experiments require a 4-node cluster with 32 A100 GPUs. Results may vary on different hardware configurations and bandwidth.
- To ensure comparable training convergence across different approaches (with relative loss error below 1e-3), we save checkpoints for each model configuration. This requires significant disk space (approximately 200 GB per model). Users can choose to train without loading checkpoints, but this may result in different routing results and loss trajectories.

B Lite Routing Algorithm

Algorithm 3: Lite Routing Algorithm

Input: $R_{rank,:}, A_{rank,:}, N, E, C, rank$: rank of current device
Output: $S_{rank,:,:}$

```

1 for each expert  $j \in [0, E - 1]$  do
2    $rep_{intra} \leftarrow$  set of replicas  $j$  intra node;
3    $rep_{inter} \leftarrow$  set of replicas  $j$  inter node;
4   if  $len(rep_{intra}) > 0$  then
5     for  $k \in rep_{intra}$  do
6        $S_{rank,j,dev_k} \leftarrow S_{rank,j,dev_k} + \frac{R_{rank,j}}{len(rep_{intra})};$ 
7   else
8     for  $k \in rep_{inter}$  do
9        $S_{rank,j,dev_k} \leftarrow S_{rank,j,dev_k} + \frac{R_{rank,j}}{len(rep_{inter})};$ 
10 return  $S_{rank,:,:};$ 

```

Here, we illustrate the lite routing algorithm used in the token dispatcher. As shown in Alg. 3, this algorithm is performed separately in each device, and for each expert, if replicas are present within a node, tokens routed to the expert are evenly distributed among all intra-node replicas (Line 5-6). In the absence of intra-node replicas, tokens are evenly allocated among all replicas across global nodes (Line 8-9).

C Expert Replica Allocation Algorithm

The replica allocation algorithm is illustrated in Alg. 4. Specifically, the algorithm maintains a priority queue (Line 2-4) that identifies the expert with the highest average load (i.e., the ratio of actual load to the number of replicas) and increases the number of replicas for that expert until the total number of replicas meets the required threshold (Line 5-8).

Algorithm 4: Replica Allocation Algorithm

Input: R, N, E, C
Output: $expert_rep$

```

1  $expert\_rep, expert\_load \leftarrow \text{ones}(E), R.sum(axis = 0);$ 
2  $priority\_queue \leftarrow \emptyset;$ 
3 for  $i \in [0, E - 1]$  do
4    $priority\_queue.push(i, \frac{expert\_load[i]}{expert\_rep[i]});$ 
5 while  $\text{sum}(expert\_rep) < N \times C$  do
6    $e \leftarrow \text{pop from } priority\_queue;$ 
7    $expert\_rep[e] \leftarrow expert\_rep[e] + 1;$ 
8    $priority\_queue.push(e, \frac{expert\_load[e]}{expert\_rep[e]});$ 
9 return  $expert\_rep;$ 

```

D Scalability Analysis

To evaluate the scalability of LAER-MoE beyond the physical constraints of our available hardware, we conducted a trace-driven simulation. This simulation utilizes real routing traces collected from the training of the Mixtral-8x7B-e8k2 model. We modeled the execution latency of the MLP module (including expert computation and All-to-All communication) under varying cluster sizes, ranging from 8 to 128 GPUs. Tab. 4 presents the simulation results. We observe that the speedup of the MLP module remains highly stable as the cluster size increases. This stability confirms that LAER-MoE scales efficiently to large-scale clusters.

Table 4. Simulated MLP Speedup of LAER-MoE on varying cluster sizes using Mixtral-8x7B-e8k2 routing traces.

Number of GPUs	MLP Speedup
8	1.491×
16	1.490×
32	1.488×
64	1.487×
128	1.482×